

Hu, L., Tang, R., Liu, Y. , Cao, Y. and Tiwari, A. (2018) Optimising the machining time, deviation and energy consumption through a multi-objective feature sequencing approach. *Energy Conversion and Management*, 160, pp. 126-140. (doi:[10.1016/j.enconman.2018.01.005](https://doi.org/10.1016/j.enconman.2018.01.005))

This is the author's final accepted version.

There may be differences between this version and the published version. You are advised to consult the publisher's version if you wish to cite from it.

<http://eprints.gla.ac.uk/155924/>

Deposited on: 23 January 2018

Enlighten – Research publications by members of the University of Glasgow  
<http://eprints.gla.ac.uk>

1

2       **Optimising the machining time, deviation and energy consumption**  
3       **through a multi-objective feature sequencing approach**

4   Luohe Hu<sup>a</sup>, Renzhong Tang<sup>a,c,\*</sup>, Ying Liu<sup>b</sup>, Yanlong Cao<sup>a,c</sup>, Ashutosh Tiwari<sup>d</sup>

5   <sup>a</sup>*State Key Laboratory of Fluid Power and Mechatronic Systems, School of Mechanical Engineering,*  
6   *Zhejiang University, Hangzhou, 310027, China*

7   <sup>b</sup>*School of Engineering, University of Glasgow, Glasgow, G12 8QQ, United Kingdom*

8   <sup>c</sup>*Key Laboratory of Advanced Manufacturing Technology of Zhejiang Province, School of Mechani-*  
9   *cal Engineering, Zhejiang University, Hangzhou, 310027, China*

10   <sup>d</sup>*Department of Automatic Control and Systems Engineering, The University of Sheffield, Sheffield,*  
11   *S1 3JD, United Kingdom*

12

13

14

15

16

17   **\*Corresponding author:** Renzhong Tang

18   **E-mail address:** tangrz@zju.edu.cn (R. Tang)

19   **Tel.:** +86(0)57187952048

20

21

22

## Optimising the machining time, deviation and energy consumption through a multi-objective feature sequencing approach

**Abstract:** A considerable amount of global energy consumption is attributable to the machining energy consumption of the machine tool. Thus, reducing the machining energy consumption can alleviate the energy crisis and energy-related environmental pollution. It has been approved that feature sequencing is an effective and economical approach to reduce the machining energy consumption. The single objective model that only minimises the machining energy consumption has been developed in previous research. However, the machining time and deviation, which are also affected by the feature sequence, have not been considered. Thus, this article first aims to understand and model the sequence-related machining time, deviation, and energy consumption (S-MT, S-MD, and S-MEC) while machining a part. Accordingly, a multi-objective feature sequencing problem, which optimises the trade-off among S-MT, S-MD, and S-MEC, is introduced. To solve it, two optimisation approaches, including Non-dominated Inserting Enumeration Algorithm (NIEA) and Non-dominated Sorting Genetic Algorithm II (NSGA-II), are proposed and employed. A case study was conducted to demonstrate the developed models and the optimisation approaches. The experiment results show that the optimal or near-optimal solution sets can be obtained for eight machine parts. By comparison, 20.51% S-MT, 5.29% S-MD, and 16.66% S-MEC can be reduced. Between the two algorithms, NIEA is recommended for the part that has fewer than 12 features. Finally, more optimisation approaches for the multi-objective problem are proposed and discussed.

**Keywords:** Machining energy; Machining deviation; Machining time; Machine tools; Feature sequencing; Multi-objective optimisation.

### Abbreviations

BTT	bottom-to-top
CNC	computer numerical control
GNEA	genetic-based non-dominated enumeration algorithm
MOEAs	multi-objective evolutionary algorithms
MOPs	multi-objective problems
NIEA	non-dominated inserting enumeration algorithm
NSGA-II	non-dominated sorting genetic algorithm II
PSFP	processing sequence of features of a part
PSFPs	processing sequences of features of a part
rpm	revolutions per minute
SI	supplementary information
S-MD	sequence-related machining deviation [ $\mu\text{m}$ ]
S-MEC	sequence-related machining energy consumption [J]
S-MP	sequence-related machining process
S-MT	sequence-related machining time [s]
S-ND	sequence-related non-cutting deviation [ $\mu\text{m}$ ]
S-NEC	sequence-related non-cutting energy consumption [J]
S-NT	sequence-related non-cutting time [s]

### Nomenclature

$\alpha_A$	angular acceleration of the spindle [ $\text{rad/s}^2$ ]
$B$	monomial coefficient in the S-ND model for the feeding activity
$d_j^{(F_p, F_q)}$	S-ND for the $j$ -th feeding activity from the feature $F_p$ to the feature $F_q$ [ $\mu\text{m}$ ]
$D_S$	total S-MD based on a specific PSFP [ $\mu\text{m}$ ]
$D_{cut}^{S_k}$	sequence-related cutting deviation for the feature at the $k$ -th position of the sequence [ $\mu\text{m}$ ]
$D_{non}^{(S_k, S_{k+1})}$	S-ND between the features at the $k$ -th and $k + 1$ -th positions of the sequence [ $\mu\text{m}$ ]
$E_{cut}^{S_k}$	sequence-related cutting energy consumption for the feature at the $k$ -th position of the sequence
$E_{non}^{(S_k, S_{k+1})}$	S-NEC between the features at the $k$ -th and $k + 1$ -th positions of the sequence [J]
$E_S$	total S-MEC based on a specific PSFP [J]
$F$	a finite set of $n + 2$ features of a part in machining environment, $F = \{F_i\}_{i=0}^{n+1}$ , $F_C \subset F$
$F_0, F_{n+1}$	virtual features to denote the start and end positions of the tool while machining a part
$F_C$	a finite set of $n$ actual features of a part, $F_C = \{F_i\}_{i=1}^n$
$F_i$	$i$ -th feature in a part
$F_p, F_q$	specific features in a part
$g$	index for the speed change of the spindle rotation
$i$	index for the feature in a part
$j$	index for the feeding activity in a tool path
$k$	index for the position in a feature sequence
$l_j^{pq}$	sequence-related non-cutting distance for the $j$ -th feeding activity between the features $F_p$ and $F_q$ [mm]
$m$	number of feeding activities in a tool path between two features
$n$	number of actual features in a part
$n_{Sg}^{pq}, n_{Eg}^{pq}$	initial and end speed of the $g$ -th speed change of the spindle rotation in the non-cutting from the feature $F_p$ to the feature $F_q$ [rpm]
$N$	population size in NSGA-II

$P_t$	parent population that is created at the $(t + 1)$ -th generation
$Q_t$	offspring population that is created at the $(t + 1)$ -th generation
$R_t$	population that is created by the combination of $P_t$ and $Q_t$ at the $(t + 2)$ -th generation
$S$	a finite set to indicate all of the positions of the features in a sequence, $S = \{S_k\}_{k=1}^{n+2}$
$S_k$	feature at the $k$ -th position of a sequence
$t$	index for the generation in NSGA-II
$t_{pj}^{(F_p, F_q)}$	time for the $j$ -th feeding activity in the non-cutting from the feature $F_p$ to the feature $F_q$ [s]
$t_{sg}^{(F_p, F_q)}$	time for the $g$ -th speed change of the spindle rotation in the non-cutting from the feature $F_p$ to the feature $F_q$ [s]
$T_{cut}^{S_k}$	sequence-related cutting time for the feature at the $k$ -th position of the sequence [s]
$T_{non}^{(S_k, S_{k+1})}$	S-NT between the features at the $k$ -th and $k + 1$ -th positions of the sequence [s]
$T_s$	total S-MT based on a specific PSFP [s]
$T_{src}^{(F_p, F_q)}$	S-NT for the spindle speed change in the non-cutting from the feature $F_p$ to the feature $F_q$ [s]
$T_{tc}^{(F_p, F_q)}$	S-NT for the tool change in the non-cutting from the feature $F_p$ to the feature $F_q$ [s]
$T_{tp}^{(F_p, F_q)}$	S-NT for the tool path in the non-cutting from the feature $F_p$ to the feature $F_q$ [s]
$u$	index for the solution in NIEA
$w$	number of speed changes of the spindle rotation between two features
$z$	natural number
$\Delta X_j^{pq}, \Delta Y_j^{pq}, \Delta Z_j^{pq}$	sequence-related relative distances of X-axis, Y-axis, and Z-axis between the start and end coordinate positions in the $j$ -th feeding activity from the feature $F_p$ to the feature $F_q$ [mm]

51

## 52 1. Introduction

53 Increasing energy price and requirements to improve energy efficiency are the new challenges faced  
54 by modern manufacturing enterprises [1]. Machine tools are widely used in manufacturing sector [2]  
55 and consume considerable amounts of energy [3]. For instance, there are over 7 million machine  
56 tools in China, whose total power can achieve 70 million kilowatts [4]. Moreover, surveys showed  
57 that the energy efficiency of machine tools is generally less than 30% [4]. Thus, reducing the energy  
58 consumption of machine tools has been identified as a potential approach to improving manufactur-  
59 ing energy efficiency [5], and it has attracted attention from both academic research and industrial  
60 applications [6].

61 Energy-aware process planning and scheduling are two effective management approaches to reduce  
62 the energy consumption of machine tools [7]. Research on energy-aware scheduling in manufactur-

ing has been well conducted [8] and achieved the target for reducing the idle energy consumption [9]. On the other hand, research on energy-aware process planning has been focused on process parameters optimisation [10] and achieved the target for reducing the machining energy consumption [11]. For example, a recent work by Shin [12] presented the novel component modelling and online optimisation of cutting parameters (feed rate, spindle speed, cutting depth and width) to minimise the milling machining energy consumption in real-time. However, energy-aware feature (operation) sequencing research is still insufficient, which restricts the energy-aware process planning.

The energy-aware feature sequencing aims at determining the processing sequence of features of a part (PSFP) that minimises the machining energy consumption of a machine tool. In existing studies, the single objective is a limitation [13]. In real manufacturing circumstance, it is not reasonable to only reduce the machining energy consumption without controlling the machining time and deviation, which can cause the problems of machine tool tardiness and product quality. In related research, Shin [12] suggested that the machining time could be considered as another objective in addition to the machining energy consumption in the formulation of an optimisation problem. However, there was an opinion that the machining time was positively correlated with the machining energy consumption [14]. As a result, the minimisation of the machining energy consumption could always result in the minimum machining time. If this opinion was true, it would be redundant to develop the machining time model. It is important to investigate this opinion. Yan [15] and Kant [16] verified the conflict between the machining quality (deviation) and energy consumption, and the machining deviation model should be developed. The lack of identification and extraction of the sequence-related machining process (S-MP) is another limitation. The S-MP is defined as the process that is affected by the PSFP. The machining time, deviation, and energy consumption for completing the S-MP are called the sequence-related machining time, deviation, and energy consumption (S-MT, S-MD, and S-MEC). Bridging the gaps and insufficiencies to model and solve the multi-objective problem has motivated this research, and the proposed solutions are the main contributions of this paper.

In our study, it is assumed that all of the required processing for a part can be finished on a single machine tool. If a part requires more than one machine tool, the features to be processed on the same machine can be sorted and separately sequenced. Besides, each feature does not have the volumetric intersection with other features. Our study aims at analysing the conflict between the S-MT and the S-MEC when processing a part, and at integrating the S-MT and S-MD models with the existing S-MEC model to obtain the multi-objective model. This article investigates a novel management approach to reduce the S-MT, S-MD, and S-MEC by merely adjusting the PSFP. The multi-objective

optimisation in this research is to achieve the optimal trade-offs among the aforementioned three objectives. A deterministic method, Non-dominated Inserting Enumeration Algorithm (NIEA), and a popular evolutionary algorithm, Non-dominated Sorting Genetic Algorithm II (NSGA-II), are proposed and used as the optimisation approaches to search for the non-dominated set of optimal solutions. Further, a novel hybrid algorithm named Genetic-based Non-dominated Enumeration Algorithm (GNEA) is proposed and compared. An optimal solution represents a PSFP that results in the optimal trade-off among the three objectives. Based on case studies, the developed models and optimisation approaches are demonstrated, compared, and discussed.

In the remainder of this paper, the literature review is presented in the next section. The problem description and the multi-objective model are given in Section 3. In Section 4, the working procedures of NIEA and NSGA-II for optimising the three objectives are described. A case study is conducted to demonstrate the multi-objective feature sequencing approach in Section 5. In Section 6, more optimisation approaches for the feature sequencing problem are analysed and discussed. Finally, a brief summary and a description of future work are given in Section 7.

## 2. Literature review

To understand and model the energy-aware feature sequencing problems, Sheng [17] developed a basic model to depict the effects of the PSFP on the machining energy consumption. Newman [18] investigated the energy-aware feature sequencing model for the computer numerical control (CNC) machining based on the experiments. Further, Hu [13] supplemented the mathematic relationship between the PSFP and the actual cutting volume of each feature in the cutting energy consumption model. However, the non-cutting energy consumption has not been provided in their models, though it accounts for a considerable portion [19]. A mathematic model was developed to describe the effects of the PSFP on the non-cutting energy consumption, including the energy of the machine tool consumed for the tool path, tool change [20], and change of spindle rotation speed [21]. In above models, there are some common limitations. Specifically, the machining energy consumption that is not affected by the PSFP has not been identified and removed, thereby leading to the redundant modelling. Single objective environment is another limitation.

The single objective model has been improved by adding the new objectives, such as the machining time and deviation [22]. In the existing multi-objective model, there are some insufficiencies on modelling the machining time, deviation, and energy consumption, which harm the model's accuracy and reliability. For example, the time and power data of the machine tool were obtained from the hy-

126 pothesis and software [23] instead of an experiment measurement [24]. Besides, the non-cutting time  
127 and energy consumption of the machine tool were assumed to be equal for different PSFPs [25]. In  
128 practice, the values of the non-cutting time and energy consumption are affected by the PSFPs, be-  
129 cause the plan of the non-cutting operations including the tool path, tool change, and change of spin-  
130 dle rotation speed can vary based on the different PSFPs [21]. In previous research, the weight was  
131 subjectively assigned to the machining time, deviation, and energy consumption [25], and the multi-  
132 objective model was transformed to a single objective model [26]. Thus, our multi-objective model  
133 aims at solving the above problems to improve its accuracy and reliability, with the support of the  
134 advanced modelling approaches for the three objectives [13].

135 After obtaining the multi-objective model, the optimisation approaches can be employed to find a set  
136 of optimal PSFPs that result in the optimal trade-offs among the minimisation of machining time,  
137 deviation, and energy consumption. The application of optimisation approaches to solve the energy-  
138 aware multi-objective feature sequencing problem can be found. For example, the standard genetic  
139 algorithm was employed to find the optimal PSFP by the weighted sum method [25], and the multi-  
140 objective optimisation problem was converted into a single objective problem. When using such a  
141 method, it has to be run many times to obtain a non-dominated set of solutions, and weak and repeat-  
142 ed solutions are usually generated [27]. Multi-objective evolutionary algorithms (MOEAs) can ob-  
143 tain a non-dominated set of solutions in a single run and are suitable for multi-objective problems  
144 (MOPs) [27]. The application of MOEAs for solving the energy-aware feature sequencing problem is  
145 scarce at present. Fortunately, MOEAs have been successfully applied to other energy-aware process  
146 planning and scheduling problems, such as process parameters optimisation [28]. These related stud-  
147 ies can be used as references for solving our problem.

148 It has been approved that NSAG-II is one of the most effective and popular MOEAs [29]. However,  
149 it is inevitable for any MOEAs to trap into the local optima, and the global optimum is not guaran-  
150 teed [27]. Thus, deterministic algorithms, which can always find the non-dominated set of Pareto-  
151 optimal solutions, have also been proposed and tested for our multi-objective problem. Specifically,  
152 NIEA is selected as a deterministic algorithm. In addition, NSGA-II is employed because it normally  
153 consumes shorter computation time to solve the medium-to-large problems than a deterministic algo-  
154 rithm does. The optimisation results and computation time of the two algorithms are compared in the  
155 case study. To obtain the global optimum more quickly for the medium-to-large problems, a novel  
156 hybrid algorithm GNEA is further proposed and discussed.



157 According to the literature reviewed, the modelling and optimisation for the aforementioned multi-  
 158 objective problem is neither sufficient nor accurate. Accordingly, our multi-objective model is im-  
 159 proved by analysing the conflict among the S-MT, the S-MD, and the S-MEC, and developing the  
 160 three objectives based on the advanced modelling approaches. Based on the improved model, this  
 161 paper investigates a novel and economical approach to optimise the trade-off among the three objec-  
 162 tives through adjusting the PSFP. Optimisation approaches based on NIEA, NSGA-II, and GNEA  
 163 are first proposed and compared to obtain the optima for our feature sequencing problem. The pro-  
 164 posed solutions for modelling and optimising the multiple objectives are the main contributions of  
 165 this paper, and they are introduced in the following sections.

### 166 3. Problem statement and modelling

167 Considering a part that has  $n$  actual features, a finite set is used for denoting these  $n$  actual features  
 168 as:

$$169 \quad F_C = \{F_i\}_{i=1}^n \quad (1)$$

170 where  $i$  is the index for the feature,  $n$  is the number of actual features in a part, and  $F_i$  is the  $i$ -th fea-  
 171 ture. Because the start and end positions of the tool also affect the S-MT, S-MD, and S-MEC, they  
 172 are defined as two virtual features for the part, denoted by  $F_0$  and  $F_{n+1}$ . Thus, in machining environ-  
 173 ment, there are  $n + 2$  features for an  $n$ -feature part, which are denoted as a finite set:

$$174 \quad F = \{F_i\}_{i=0}^{n+1}. \quad (2)$$

175 Obviously, the  $F_C$  is a subset of the  $F$  ( $F_C \subset F$ ). In terms of optimisation, the aim of this research is  
 176 to determine the non-dominated set of optimal PSFPs that result in the optimal trade-offs among S-  
 177 MT, S-MD, and S-MEC under the precedence constraints.

178 The conflict between the machining deviation and energy consumption was verified in the previous  
 179 study [15], and our paper investigates the relationship between the machining time and energy con-  
 180 sumption. In **Fig. 1**, a part that has two actual features (holes) is used as an example to explain the S-  
 181 MT, the S-MEC, and the possible conflict between them. The two features are denoted as  $F_1$  and  $F_2$ ,  
 182 and they are processed by two different spindle rotation speeds of 500rpm and 800rpm. The start and  
 183 end positions of the tool, which are virtual features, are denoted as  $F_0$  and  $F_3$ . Two sequences of the  
 184 features can be used to process this part:  $F_0-F_1-F_2-F_3$  and  $F_0-F_2-F_1-F_3$ . The tool paths of the two se-  
 185 quences are labelled by blue solid lines and red dashed lines, respectively, in **Fig. 1**. In particular, the

actual tool paths between  $B$  and  $C$ ,  $B$  and  $D$ , and  $D$  and  $E$  are straight lines instead of curves, and the distances from  $B$  to  $H$  and from  $D$  to  $H$  are equal. The power profiles of a machine tool when processing the part according to the aforementioned two sequences are shown in **Fig. 2**. The power profiles are developed based on the measured data [30] and the prediction method [31].

**Fig. 1.** A two-feature part that has two possible processing sequences.

The first step is to determine the S-MP. The S-MP is identified by checking whether a machining process (feeding activity) exists in all of the PSFPs or not. If it does not, the machining process is sequence-related, and reserved. Otherwise, the machining process is not sequence-related, and deleted. For example, the machining processes from  $A$  to  $B$ , from  $B$  to  $D$ , and from  $D$  to  $H$  do not exist in both of the two PSFPs, as shown in **Fig. 1**, thus these processes are sequence-related, and reserved. The machining processes from  $B$  to  $C$  to  $B$  and from  $D$  to  $E$  to  $D$  exist in both of the two PSFPs, thus these processes are not sequence-related, and deleted, as shown in **Fig. 1**. Further, the corresponding machining energy consumption is removed, and filled with blank in **Fig. 2**. The machining time and energy consumption for the S-MP are namely the S-MT and S-MEC. The S-MEC for the  $F_0-F_1-F_2-F_3$  and the  $F_0-F_2-F_1-F_3$  are filled with forward blue slashes and red nets, respectively, in **Fig. 2**. The effect of the PSFP on the S-MT and the S-MEC can be found in Hu [21].

**Fig. 2.** Power profiles of two different sequences: (a)  $F_0-F_1-F_2-F_3$ ; (b)  $F_0-F_2-F_1-F_3$ .

The possible conflict between the S-MT and the S-MEC is analysed. Specifically, the distance of the tool path from  $A$  to  $B$  is shorter than that from  $A$  to  $D$ , and the distances of the other tool paths are equal. Thus, the S-MT for the  $F_0-F_1-F_2-F_3$  is shorter than that for the  $F_0-F_2-F_1-F_3$ . Prior to the final tool path, the S-MEC for the  $F_0-F_1-F_2-F_3$  is probably smaller than that for the  $F_0-F_2-F_1-F_3$ , as reflected by the size of forward blue slashes and red nets in **Fig. 2**. The spindle rotation speed during the final tool path from  $D$  to  $H$  (800rpm) is higher than that from  $B$  to  $H$  (500rpm), and the power of the machine tool increases with the spindle rotation speed [32]. Consequently, the total S-MEC for the  $F_0-F_1-F_2-F_3$  can be higher than that for the  $F_0-F_2-F_1-F_3$  when the point  $H$  is far enough to  $B$  and  $D$ . Hence, this example shows the theoretical possibility that the shorter S-MT can result in the higher S-MEC for a PSFP.

In this paper, the dimension error is used as the index for evaluating the machining deviation. The S-MD is not positively correlated with the S-MT and the S-MEC. In other words, the reductions of S-MT and S-MEC may result in the increase of S-MD. The conflict among the three objectives is test-

216 ed and verified in the following case study. Thus, it is required to develop the multi-objective model  
 217 for optimising the trade-offs among S-MT, S-MD, and S-MEC.

218 Following the example, the multi-objective model for an  $n$ -feature part is developed. Because there  
 219 are  $n + 2$  features for an  $n$ -feature part in machining environment, a finite set is employed to indicate  
 220 the positions of the features in a sequence as:

$$221 \quad S = \{S_k\}_{k=1}^{n+2} \quad (3)$$

222 where  $k$  is the index for the position in a feature sequence and  $S_k$  indicates the feature at the  $k$ -th po-  
 223 sition of a sequence. For example,  $S_k = F_p$  indicates that the feature at the  $k$ -th position is the feature  
 224  $F_p$ . For any part, the feature at the 1-st and  $n + 2$ -th position is  $F_0$  ( $S_1 = F_0$ ) and  $F_{n+1}$  ( $S_{n+2} = F_{n+1}$ ),  
 225 respectively. The total S-MT and S-MEC based on a specific PSFP can be divided into the sequence-  
 226 related non-cutting and cutting time and energy consumption. It is assumed that the S-MD for a  
 227 PSFP is accumulated by the cutting and non-cutting deviations of each feature. Thus, the multi-  
 228 objective function can be expressed as follows:

$$229 \quad \begin{cases} \text{minimise } T_s = \sum_{k=1}^{n+1} T_{non}^{(S_k, S_{k+1})} + \sum_{k=2}^{n+1} T_{cut}^{S_k} \\ \text{minimise } D_s = \sum_{k=1}^{n+1} D_{non}^{(S_k, S_{k+1})} + \sum_{k=2}^{n+1} D_{cut}^{S_k} \\ \text{minimise } E_s = \sum_{k=1}^{n+1} E_{non}^{(S_k, S_{k+1})} + \sum_{k=2}^{n+1} E_{cut}^{S_k} \end{cases} \quad (4)$$

230 where  $T_s$ ,  $D_s$ , and  $E_s$  are the total S-MT, S-MD, and S-MEC, respectively, based on a specific PSFP;  
 231  $T_{non}^{(S_k, S_{k+1})}$ ,  $D_{non}^{(S_k, S_{k+1})}$ , and  $E_{non}^{(S_k, S_{k+1})}$  are the sequence-related non-cutting time, deviation, and energy  
 232 consumption (S-NT, S-ND, and S-NEC), respectively, between the features at the  $k$ -th and  $k + 1$ -th  
 233 positions of the sequence;  $T_{cut}^{S_k}$ ,  $D_{cut}^{S_k}$ , and  $E_{cut}^{S_k}$  are the sequence-related cutting time, deviation, and  
 234 energy consumption, respectively, for the feature at the  $k$ -th position of the sequence.

235 In this presented paper, it is assumed that each feature in the part does not have the volumetric inter-  
 236 section with any other features. Consequently, the values of the cutting time, deviation, and energy  
 237 consumption for all features keep equal whatever the PSFP is [21]. Thus, the cutting time, deviation,  
 238 and energy consumption are not sequence-related, and  $T_{cut}^{S_k}$ ,  $D_{cut}^{S_k}$ , and  $E_{cut}^{S_k}$  are set to zero. Then, Ex-  
 239 pression (4) can be simplified as:

$$\begin{cases} \text{minimise } T_s = \sum_{k=1}^{n+1} T_{non}^{(S_k, S_{k+1})} \\ \text{minimise } D_s = \sum_{k=1}^{n+1} D_{non}^{(S_k, S_{k+1})} \\ \text{minimise } E_s = \sum_{k=1}^{n+1} E_{non}^{(S_k, S_{k+1})} \end{cases} \quad (5)$$

The feature at the  $k$ -th and  $k + 1$ -th position is  $F_p$  ( $S_k = F_p$ ) and  $F_q$  ( $S_{k+1} = F_q$ ), respectively. The non-cutting time of the machine tool can consist of the time consumed for the tool path, tool change, and spindle speed change [21]. Then,  $T_{non}^{(S_k, S_{k+1})}$  can be expressed as:

$$T_{non}^{(S_k, S_{k+1})} = T_{non}^{(F_p, F_q)} = T_{tp}^{(F_p, F_q)} + T_{tc}^{(F_p, F_q)} + T_{src}^{(F_p, F_q)} \quad (6)$$

where  $T_{tp}^{(F_p, F_q)}$ ,  $T_{tc}^{(F_p, F_q)}$ , and  $T_{src}^{(F_p, F_q)}$  are the S-NT for the tool path, tool change, and spindle speed change, respectively, in the non-cutting from the feature  $F_p$  to the feature  $F_q$ .

A tool path from  $F_p$  to  $F_q$  can consist of  $m$  sequential feeding activities [20], and the time for the  $j$ -th feeding activity is denoted as  $t_{pj}^{(F_p, F_q)}$ . Thus,  $T_{tp}^{(F_p, F_q)}$  can be expressed as:

$$T_{tp}^{(F_p, F_q)} = \sum_{j=1}^m t_{pj}^{(F_p, F_q)}. \quad (7)$$

Before calculating  $t_{pj}^{(F_p, F_q)}$ , it checks whether the feeding activity is sequence-related or not. If not sequence-related, then  $t_{pj}^{(F_p, F_q)} = 0$ . For example, in **Fig. 1**, the feeding activity from  $C$  to  $B$  is the 1-st feeding activity in the tool path from  $F_1$  to  $F_2$  and it is not sequence-related, thus  $t_{p1}^{(F_1, F_2)} = 0$ . If sequence-related, then  $t_{pj}^{(F_p, F_q)}$  is calculated according to its feeding approaches (rapid and normal), and the calculation method can be found in Hu [20].

Before calculating  $T_{tc}^{(F_p, F_q)}$  in Expression (6), it checks whether the tool change is sequence-related or not. If not sequence-related, then  $T_{tc}^{(F_p, F_q)} = 0$ . Otherwise, the value of  $T_{tc}^{(F_p, F_q)}$  is calculated according to the number of tool stations rotated for changing tools [33].

In the non-cutting from  $F_p$  to  $F_q$ , the spindle rotation speed can change more than one time. Thus, in Expression (6),  $T_{src}^{(F_p, F_q)}$  can be expressed as:

$$T_{src}^{(F_p, F_q)} = \sum_{g=1}^w t_{sg}^{(F_p, F_q)} \quad (8)$$

261 where  $t_{sg}^{(F_p, F_q)}$  is the time for the  $g$ -th speed change of the spindle rotation in the non-cutting from  $F_p$   
 262 to  $F_q$ ,  $w$  is the number of speed changes of the spindle rotation, and  $g$  is the index for a speed change  
 263 of the spindle rotation. It checks whether the speed change of the spindle rotation is sequence-related  
 264 or not. If not sequence-related, then  $t_{sg}^{(F_p, F_q)} = 0$ . Otherwise,  $t_{sg}^{(F_p, F_q)}$  is calculated as:

$$265 \quad t_{sg}^{(F_p, F_q)} = \frac{2\pi(n_{Eg}^{pq} - n_{sg}^{pq})}{60\alpha_A} \quad (9)$$

266 where  $n_{sg}^{pq}$  and  $n_{Eg}^{pq}$  are the initial and end speed of the  $g$ -th speed change of the spindle rotation  
 267 [rpm], and  $\alpha_A$  is the angular acceleration of the spindle [rad/s<sup>2</sup>].

268 In Expression (5),  $D_{non}^{(S_k, S_{k+1})}$  consists of the S-ND for  $m$  sequential feeding activities [20], and the S-  
 269 ND for the  $j$ -th feeding activity is denoted as  $d_j^{(F_p, F_q)}$ . Then,  $D_{non}^{(S_k, S_{k+1})}$  can be expressed as:

$$270 \quad D_{non}^{(S_k, S_{k+1})} = D_{non}^{(F_p, F_q)} = \sum_{j=1}^m d_j^{(F_p, F_q)}. \quad (10)$$

271 It is assumed that the machining deviation has a positive linear correlation with the machining dis-  
 272 tance. Then,  $d_j^{(F_p, F_q)}$  can be expressed as:

$$273 \quad d_j^{(F_p, F_q)} = B \times l_j^{pq} \quad (11)$$

274 where  $l_j^{pq}$  is the sequence-related non-cutting distance for the  $j$ -th feeding activity between the fea-  
 275 tures  $F_p$  and  $F_q$  [mm]; coefficient  $B$  can be obtained by linear regression based on experiment data.  
 276 For the three-axis CNC machine tools, the  $l_j^{pq}$  can be calculated by [32]:

$$277 \quad l_j^{pq} = \sqrt{(\Delta X_j^{pq})^2 + (\Delta Y_j^{pq})^2 + (\Delta Z_j^{pq})^2} \quad (12)$$

278 where  $\Delta X_j^{pq}$ ,  $\Delta Y_j^{pq}$ , and  $\Delta Z_j^{pq}$  are the sequence-related relative distances of X-axis, Y-axis, and Z-axis  
 279 between the start coordinate position  $(x_{j-1}^{pq}, y_{j-1}^{pq}, z_{j-1}^{pq})$  and the end coordinate position  $(x_j^{pq}, y_j^{pq},$   
 280  $z_j^{pq})$  for the  $j$ -th feeding activity. Before calculating  $\Delta X_j^{pq}$ ,  $\Delta Y_j^{pq}$ , and  $\Delta Z_j^{pq}$ , it checks whether the  
 281 relative distance at the corresponding axis is sequence-related or not. The calculation for  $\Delta X_j^{pq}$  is  
 282 taken as example. If not sequence-related, then  $\Delta X_j^{pq} = 0$ . Otherwise,  $\Delta X_j^{(F_p, F_q)} = |x_j^{pq} - x_{j-1}^{pq}|$ .

283 In Expression (5),  $E_{non}^{(S_k, S_{k+1})}$  is modelled based on the identification of the S-MP and the models in  
 284 Hu [21].

285 The constraint equations of the model are developed according to the precedence constraints among  
 286 the features [34]. For example, one of the precedence constraints is that a feature  $F_p$  should be pro-  
 287 cessed prior to a feature  $F_q$ , and then the constraint equation can be expressed as:

$$288 \quad \begin{cases} S_k = F_p \\ S_{k+z} = F_q \\ z \geq 1 \end{cases} \quad (13)$$

289 where  $z$  is a natural number. A feasible PSFP (solution) should satisfy all of the constraint equations.  
 290 The S-MT, the S-MD, and the S-MEC for the corresponding PSFP are set to infinity “ $\infty$ ” once any  
 291 feature and its pre- or post- features in a sequence violate any constraint equation.

#### 292 **4. Multi-objective optimisation**

293 After developing the multi-objective (S-MT, S-MD, and S-MEC) model, the optimisation approach-  
 294 es such as deterministic algorithms and evolutionary algorithms can be employed to obtain the non-  
 295 dominated set of optimal solutions. According to the number of features in a part, suitable optimisa-  
 296 tion approaches can be selected. Normally, deterministic algorithms are used for the part with a small  
 297 number of features, and evolutionary algorithms are used for the part with a large number of features.  
 298 In existing research, the approach to clearly define the number of features as “small” or “large” has  
 299 not been provided.

300 In single objective (S-MT) optimisation, Wiener [35] presented that the computation time of deter-  
 301 ministic algorithms was short when the number of features in a part was fewer than 14. Thus, the  
 302 number of features fewer than 14 could be defined as “small”. When the number of features in-  
 303 creased to 20, the computation time of deterministic algorithms was intolerant [34]. Thus, the num-  
 304 ber of features more than 20 could be defined as “large”. Should the number of features between 14  
 305 and 20 be defined as “small” or “large”? Experiments are conducted in Section 5 to define them ac-  
 306 cording to the computation time.

307 The multi-objective model is more complex than the single objective (S-MT) model, thereby increas-  
 308 ing its computation time. As a result, the number of features fewer than 14 is probably classified as  
 309 “large” in the multi-objective optimisation for its long computation time.

#### 4.1. Optimisation for the part with a small number of features

When the number of features in a part is small, the total number of feasible PSFPs will not be large. The S-MT, S-MD, and S-MEC for all feasible PSFPs can be enumerated, calculated, and compared in a short time. Non-dominated Inserting Enumeration Algorithm (NIEA) is proposed to optimise the three objectives for the part with a small number of features. As a deterministic approach, NIEA can accurately find the global optimal solution set in each run. According to the flowchart of NIEA in **Fig. 3**, the working procedures for solving the multi-objective problem are as follows.

**Fig. 3.** Flowchart of NIEA.

Step 1: The index  $u$  for the solution (PSFP) is initialised to 1. According to Expression (2) and lexicographical order [36], the 1-st solution is generated. If the solution does not satisfy Equation (13), it is illegal and eliminated. Otherwise, the solution is inserted into the non-dominated set.

Step 2: The index is operated by  $u = u + 1$ , and the  $u$ -th solution is generated according to Expression (2) and lexicographical order.

Step 3: The legality of the  $u$ -th solution is checked. If the  $u$ -th solution does not satisfy Equation (13), it is illegal and eliminated. Otherwise, Step 4 is performed.

Step 4: The  $u$ -th solution is verified and inserted into the non-dominated set based on the non-dominated inserting operator. The non-dominated inserting operator is performed as follows. If the  $u$ -th solution is non-dominated by all solutions in the current non-dominated set, the  $u$ -th solution is inserted into the set, and the solutions dominated by the  $u$ -th solution are removed from the set. Otherwise, the  $u$ -th solution itself is eliminated. For this operator, the rule for comparing two solutions is as follows. If any objective value among S-MT, S-MD, and S-MEC of the solution X is greater than that of the solution Y and the other two objectives values of the solution X are not smaller than those of the solution Y, the solution X is dominated by (inferior to) solution Y. Otherwise, the solution X is non-dominated by (not inferior to) the solution Y. The objectives values are calculated by Expression (5).

Step 5: NIEA checks whether the stopping conditions have been met or not. If the stopping conditions are met, all of the solutions (PSFPs) in the latest non-dominated set and their values of S-MT, S-MD, and S-MEC are reported, and NIEA stops. Otherwise, NIEA returns to Step 2. The index is

operated again by  $u = u + 1$ , and the next solution is generated and verified. The stopping conditions can be that the  $u$ -th solution has been the end of the lexicographical order.

The performance of NIEA for optimising the parts with different number of features is tested in Section 5.

#### 4.2. Optimisation for the part with a large number of features

In real manufacturing environment, the complex parts normally have more than 20 features. If still using NIEA, its computation time will be intolerant. As one of the most popular and effective non-dominated sorting-based MOEAs [29], NSGA-II normally consumes much less time to obtain a satisfying solution set [37] for the medium-to-large problems [38]. Thus, NSGA-II is used for the part with a large number of features. However, NSAG-II can be easily trapped into the local optima, and finding the global optimal solution set is not guaranteed [29]. Hence, experiments are conducted in Section 5 to test the performance of NSGA-II in the solution quality. According to the flowchart of NSGA-II in **Fig. 4**, the working procedures for solving the multi-objective problem are as follows.

**Fig. 4.** Flowchart of NSGA-II.

Step 1: The PSFP is encoded. According to Expression (2), the features to be encoded are collected. According to Expression (3), the PSFPs are obtained. Each PSFP is encoded to a chromosome by integer coding [39]. Each gene in the chromosome represents a specific feature. For example, a PSFP  $F_0-F_5-F_7-F_3-F_6-F_1-F_4-F_2-F_8$  can be encoded to a chromosome [057361428]. The gene 3 represents the feature  $F_3$ .

Step 2: An initial population  $P_0$  that has  $N$  chromosomes is randomly generated. If the gene sequence in a chromosome does not satisfy Equation (13), the corresponding chromosome is illegal. Then, the gene sequence in the illegal chromosome is adjusted according to precedence constraints until Equation (13) has been met.

Step 3: All chromosomes in the population  $P_0$  are ranked using two sorting procedures [27]: 1) a non-dominated sorting procedure and 2) a crowding distance sorting procedure. The details about the two sorting procedures can be referred to Deb [27]. In general, the chromosomes with the smaller S-MT, S-MD, and S-MEC have the higher rank (fitness), and the three objectives values are calculated according to Expression (5).



Step 4: The offspring population  $Q_0$  is generated. At the 1-st generation, the GA operators, including the selection, crossover, and mutation, create the offspring population  $Q_0$  of  $N$  chromosomes. The selection operator aims at selecting chromosomes in the current generation to reproduce offspring. A binary tournament is adopted as the selection operator: between two chromosomes, the one with the higher rank is selected [1]. The rank of each chromosome is determined as follows: the chromosomes on the lower non-dominated level have the absolute higher rank; on the same non-dominated level, the chromosomes with the greater value in the crowding distance have the higher rank [1]. More details about this selection operator can be referred to Blickle [40]. The partially mapped crossover [41] and the swap mutation [1] are adopted as the crossover operator and the mutation operator, respectively, and more details can be referred to Goldberg [41] and Liu [1].

Step 5: The generation number is operated by  $t = t + 1$ . At the  $t$ -th ( $t \geq 2$ ) generation, the parent population  $P_{t-2}$  and its offspring population  $Q_{t-2}$  are combined to create a new population as  $R_{t-2}$  with a size of  $2N$ . The  $2N$  chromosomes in the  $R_{t-2}$  are also ranked using the aforementioned two sorting procedures. The  $N$  chromosomes with the highest rank are selected from the  $R_{t-2}$  to form the new parent population  $P_{t-1}$ .

Step 6: The new offspring population  $Q_{t-1}$  that has  $N$  chromosomes is created through the selection, crossover, and mutation operators.

Step 7: NSGA-II checks whether the stopping conditions have been met or not. If the stopping condition is met, the final population is decoded to report the set of optimal PSFPs that result in the optimal trade-offs among S-MT, S-MD, and S-MEC, and NSGA-II stops. Otherwise, NSGA-II returns to Step 5. The generation number is operated by  $t = t + 1$ , and the next population is created. This generational process is repeated until a stopping condition has been met [42]. The stopping condition can be the specified maximum generation number that is reached.

## 5. Case study

### 5.1. Case description, modelling, and optimisation

Three parts are used as the case studies to demonstrate the developed multi-objective models and optimisation approaches. Both part A and part B have 8 actual features (holes) denoted by  $F_1 - F_8$  and 2 virtual features ( $F_0$  and  $F_9$ ), as shown in **Figs. 5** and **6**. The surfaces  $X$  and  $Y$  are selected as the primary positioning reference for part A, as marked in **Fig. 5**. Part C has 14 actual features denoted by

395  $F_1 - F_{14}$  and 2 virtual features ( $F_0$  and  $F_{15}$ ), as shown in **Fig. 7**. In parts A, B, and C, each feature  
 396 does not have volumetric intersections with the other features, and there is no specific constraint on  
 397 the PSFP. A vertical machining centre (XHF-714F) manufactured by Hangzhou CNC Machine Tool  
 398 Co., Ltd. of China is used to process the three parts. The experiment setup for the power data collec-  
 399 tion on the XHF-714F is shown in **Fig. 8**. The key parameters of the XHF-714F required for calculat-  
 400 ing the S-MT and the S-MEC are listed in Hu [21]. The coefficient  $B$  in the S-MD model is:  $B =$   
 401  $0.001$ . They have been obtained through experiment measurement and regression analysis [32]. The  
 402 spindle rotation speeds for each feature in parts A, B, and C are listed in **Table 1**, and the feed rates  
 403 for all of the features are  $0.09\text{mm/rev}$ . They have been obtained from the process files. On the basis  
 404 of the above and additional case information provided in Hu [21], the S-MT, the S-MD, and the S-  
 405 MEC can be calculated.

406 **Fig. 5.** Part A with 8 actual features and 2 virtual features.

407 **Fig. 6.** Part B with 8 actual features and 2 virtual features.

408 **Fig. 7.** Part C with 14 actual features and 2 virtual features.

409 **Fig. 8.** Diagram of the experiment setup for power data acquisition.

410 **Table 1** Spindle rotation speeds for the features in parts A, B, and C.

411 For parts A and B with 10 features, considering the position of the 2 virtual features on the sequence  
 412 ( $S_1 = F_0$ ,  $S_{10} = F_9$ ), there are 81  $[(10-1)*(10-1)]$  possible pairs of features. Similarly, there are 225  
 413  $[(16-1)*(16-1)]$  pairs of features for part C. In the following, the value calculation procedures for the  
 414 S-NT, the S-ND, and the S-NEC between processing  $F_2$  and  $F_6$  ( $T_{non}^{(F_2, F_6)}$ ,  $D_{non}^{(F_2, F_6)}$ , and  $E_{non}^{(F_2, F_6)}$ ) in part  
 415 A are used as examples.

416 Based on the above and Expression (6), the S-NT from  $F_2$  to  $F_6$  is:

$$417 \quad T_{non}^{(F_2, F_6)} = T_{tp}^{(F_2, F_6)} + T_{tc}^{(F_2, F_6)} + T_{src}^{(F_2, F_6)}$$

418 where  $E_{tp}^{(F_2, F_6)}$ ,  $E_{tc}^{(F_2, F_6)}$ , and  $E_{src}^{(F_2, F_6)}$  are the S-NT for the tool path, tool change, and spindle speed  
 419 change, respectively, in the non-cutting process from  $F_2$  to  $F_6$ .

420 There are three feeding activities in the non-cutting from  $F_2$  to  $F_6$ , as shown in **Fig. 5**. Thus,  $T_{tp}^{(F_2, F_6)}$   
 421 can be expressed as:  $T_{tp}^{(F_2, F_6)} = t_{p1}^{(F_2, F_6)} + t_{p2}^{(F_2, F_6)} + t_{p3}^{(F_2, F_6)}$ .  
 422 As shown in **Fig. 5**, the 1-st feeding activity (from  $A$  to  $B$ ) and the 3-rd feeding activity (from  $C$  to  $D$ )  
 423 are not sequence-related, thus  $t_{p1}^{(F_2, F_6)} = 0s$  and  $t_{p3}^{(F_2, F_6)} = 0s$ . The 2-nd feeding activity (from  $B$  to  $C$ )  
 424 is sequence-related, thus  $t_{p2}^{(F_2, F_6)}$  is calculated as follows. The feeding approach from  $B$  to  $C$  is rapid  
 425 feeding, and the coordinates of the points  $B$  and  $C$  are (0, 60, 7) and (25, 15, 7), respectively. Based  
 426 on the time model for rapid feeding in Hu [20], the value of  $t_{p2}^{(F_2, F_6)}$  is 0.225s. Then,  $T_{tp}^{(F_2, F_6)}$  is calcu-  
 427 lated as:  $T_{tp}^{(F_2, F_6)} = 0 + 0.225 + 0 = 0.225s$ .

428 In the non-cutting from  $F_2$  to  $F_6$ , there is no tool change, thus  $T_{tc}^{(F_2, F_6)} = 0s$ .

429 There is only one speed change of the spindle rotation within this case. According to Expression (8),  
 430  $E_{src}^{(F_2, F_6)}$  is expressed as:  $T_{src}^{(F_2, F_6)} = t_{s1}^{(F_2, F_6)}$ . The spindle rotation speeds for  $F_2$  and  $F_6$  are 550rpm and  
 431 800rpm according to **Table 1**, thus  $n_{s1}^{26} = 550rpm$  and  $n_{E1}^{26} = 800rpm$ . The angular acceleration is  
 432  $1047.20rad/s^2$ . Then, Equation (9) is employed to calculate  $t_{s1}^{(F_2, F_6)}$  as:  $t_{s1}^{(F_2, F_6)} = \frac{2\pi \times (800 - 550)}{60 \times 1047.20} =$   
 433  $0.025s$ .

434 By summing  $T_{tp}^{(F_2, F_6)}$ ,  $T_{tc}^{(F_2, F_6)}$ , and  $T_{src}^{(F_2, F_6)}$ , the S-NT from  $F_2$  to  $F_6$  is:

$$435 T_{non}^{(F_2, F_6)} = 0.225 + 0 + 0.025 = 0.250s.$$

436 According to Expression (10), the S-ND from  $F_2$  to  $F_6$  is:

$$437 D_{non}^{(F_2, F_6)} = d_1^{(F_2, F_6)} + d_2^{(F_2, F_6)} + d_3^{(F_2, F_6)}.$$

438 As shown in **Fig. 5**, the 1-st feeding activity and the 3-rd feeding activity are not sequence-related,  
 439 thus  $d_1^{(F_2, F_6)} = 0\mu m$  and  $d_3^{(F_2, F_6)} = 0\mu m$ . The 2-nd feeding activity (from  $B$  to  $C$ ) is sequence-related.  
 440 The coordinates of the points  $B$  and  $C$  are (0, 60, 7) and (25, 15, 7), respectively. The relative dis-  
 441 tance at the  $Z$ -axis axis is not sequence-related. According to Expressions (11)-(12) and coefficient  
 442  $B = 0.001$ ,  $d_2^{(F_2, F_6)}$  is calculated as:

$$443 d_2^{(F_2, F_6)} = 0.001 \times \sqrt{(25)^2 + (-45)^2 + (0)^2} = 51.48\mu m.$$

444 Finally,  $D_{non}^{(F_2, F_6)}$  is:  $D_{non}^{(F_2, F_6)} = 0 + 51.48 + 0 = 51.48\mu\text{m}$ .

445 Based on the identification of the S-MP and the models in Hu [21], the value of  $E_{non}^{(F_2, F_6)}$  is 438.89J.

446 Following the calculations of  $T_{non}^{(F_2, F_6)}$ ,  $D_{non}^{(F_2, F_6)}$ , and  $E_{non}^{(F_2, F_6)}$ , the S-NT, the S-ND, and the S-NEC for  
447 the other 80 pairs of features in part A are calculated based on the similar procedures, and the results  
448 are listed in **Tables 2, 3, and 4**. In addition, the S-NT and the S-NEC for 81 and 225 pairs of features  
449 in parts B and C are provided in **Tables S1, S2, S3, and S4** of the Supplementary Information (SI).  
450 To test the conflict between the S-NT and the S-NEC, the S-ND for parts B and C is set to zero. In  
451 this case, the feeding approach for all sequence-related feeding activities is rapid feeding. The rapid  
452 feeding speeds of the X-axis, the Y-axis, and the Z-axis of the machine tool (XHF-714F) are high,  
453 which are 12m/min, 12m/min, and 10m/min, respectively. Thus, the values of the S-NT between the  
454 features in the three parts are small.

455 **Table 2** S-NT for 81 pairs of features in part A.

456 **Table 3** S-ND for 81 pairs of features in part A.

457 **Table 4** S-NEC for 81 pairs of features in part A.

458 Based on the data and models above and the supplementary tables in the SI, two solution algorithms,  
459 NIEA and NSGA-II, are employed as optimisation approaches. In this research, NIEA and NSGA-II  
460 are developed on Dev C++ 5.11.0 software with the programming language C++. The C++ code of  
461 NIEA can be found at the SI. The computing platform is Intel (R) Core (TM) i7-2630 QM CPU with  
462 2.00 GHz frequency; 4.00 GB RAM; Windows 7 (64bit) operating system. The parameter values  
463 used in NSGA-II are obtained by fine tuning, and their values are as follows: population size = 50;  
464 crossover probability = 0.9; mutation probability = 0.15; generation number = 100 (parts A and B)  
465 or 200 (part C).

466 The S-MD is set to zero first. NIEA and NSGA-II are run 10 times for parts A, B, and C, respective-  
467 ly, according to standard deviation. The results from using NIEA and NSGA-II for optimising the  
468 feature sequences of these parts are summarised and compared in **Table 5** and **Figs. 9, 10, and 11**. As  
469 a deterministic algorithm, NIEA can always obtain the non-dominated set of Pareto-optimal solutions  
470 for parts A, B, and C. The results are listed in **Table 5**, including the set of the optimal PSFPs and  
471 their objectives values. In particular, there is only one solution for part B, and it means the PSFP with

the minimum S-MEC also results in the minimum S-MT. The optimal solution sets for parts A, B, and C obtained by NIEA are also shown in **Figs. 9, 10, and 11.**

**Table 5** The results obtained by BTT and NIEA for parts A, B, and C.

**Fig. 9.** Comparison of solution quality between NIEA and NSGA-II for part A.

**Fig. 10.** Comparison of solution quality between NIEA and NSGA-II for part B.

**Fig. 11.** Comparison of solution quality between NIEA and NSGA-II for part C.

Then, the S-MD for part A is set to the values in **Table 3**, and NIEA is employed to find the set of optimal solutions (PSFPs) that result in the optimal trade-offs among S-MT, S-MD, and S-MEC. The solution set of part A is listed in **Table 6**, and its computation time is 0.1763s. It demonstrates that the reduction of S-MD can result in the increase of S-MT and S-MEC.

**Table 6** The solutions obtained by NIEA for the multi-objective model of part A.

## 5.2. Results and analysis

To demonstrate the effectiveness of the proposed approaches in reducing the S-MT, the S-MD, and the S-MEC, the following comparison is performed. A feature sequence produced by the sequencing technique Bottom-to-Top (BTT) [43] serves as the benchmark to represent the traditional approach to arranging the PSFP. Then, the benchmark PSFP for parts A, B, and C is  $F_0 - F_1 - F_5 - F_6 - F_7 - F_4 - F_3 - F_2 - F_8 - F_9$ ,  $F_0 - F_4 - F_5 - F_8 - F_3 - F_1 - F_6 - F_7 - F_2 - F_9$ , and  $F_0 - F_4 - F_{14} - F_6 - F_5 - F_{11} - F_{10} - F_7 - F_1 - F_3 - F_9 - F_8 - F_{12} - F_{13} - F_2 - F_{15}$ , respectively. Based on the data in **Table 2**, **Table 4**, and supplementary tables in the SI, the S-MT and the S-MEC for the benchmark PSFPs are calculated and listed in **Table 5**. According to **Table 3**, the S-MD based on the benchmark PSFP for part A is 553.28 $\mu$ m.

By comparing the S-MT and S-MEC values in **Table 5**, 23.00% [(4.022-3.097)/4.022] to 25.41% [(4.022-3.000)/4.022] S-MT and 19.47% [(6321.99-5091.26)/6321.99] to 22.33% [(6321.99-4910.49)/6321.99] S-MEC are reduced for part A; 33.13% [(3.737-2.499)/3.737] S-MT and 26.86% [(5790.27-4235.01)/5790.27] S-MEC are reduced for part B; 39.14% [(6.728-4.095)/6.728] to 41.90% [(6.728-3.909)/6.728] S-MT and 33.68% [(9871.92-6547.28)/9871.92] to 38.36% [(9871.92-6085.46)/9871.92] S-MEC are reduced for part C. The results verify the conflict between the minimisation of S-MT and S-MEC. According to the processing constraints for the S-MT, the optimal

PSFP can be selected from the solution set. For example, the S-MT for parts A and C is restrained to be not longer than 3.000 and 4.000 seconds, respectively. Thus, the 1-st sequence  $F_0 - F_6 - F_8 - F_7 - F_4 - F_2 - F_3 - F_5 - F_1 - F_9$  and the 3-rd sequence  $F_0 - F_1 - F_7 - F_8 - F_2 - F_9 - F_{10} - F_3 - F_{13} - F_{12} - F_{11} - F_{14} - F_6 - F_4 - F_5 - F_{15}$  are selected for parts A and C, as shown in **Figs. 5** and **7**, because they consume the minimum S-MEC under the S-MT constraints.

By comparing the three objectives values generated by NIEA and BTT according to **Table 6**, 20.51% [(4.022-3.197)/4.022] to 25.41% [(4.022-3.000)/4.022] S-MT, 5.29% [(553.28-524.01)/553.28] to 27.90% [(553.28-398.92)/553.28] S-MD, and 16.66% [(6321.99-5268.75)/6321.99] to 22.33% [(6321.99-4910.49)/6321.99] S-MEC are reduced for part A through the multi-objective optimisation.

Further, the performances between the two algorithms (NIEA and NSGA-II) for parts A, B, and C are compared and summarised in **Table 7**. The deterministic algorithm, NIEA, can always return the global optimum. By comparison, NSGA-II can find an optimal or near-optimal solution set. Particularly, NSGA-II obtained the global optimum for part B sometimes, but it has never obtained the global optimum for parts A and C in our trials.

**Table 7** Performance comparison between NIEA and NSGA-II for parts A, B, and C.

The hypervolume indicator is employed to evaluate the solution quality of the two algorithms [44]. The maximum objectives values of the 10 trials are taken as the coordinate values of the reference point. Then, the reference points of parts A, B, and C are A(3.098, 5111.05), B(2.585, 4398.92), and C(4.205, 6560.02), respectively, as shown in **Figs. 9, 10, and 11**. Based on the reference points and the objectives values of the solutions, the hypervolume indicator of NIEA and NSGA-II for parts A, B, and C can be obtained by calculating the size of the dominated subspaces. In **Figs. 9, 10, and 11**, the spaces surrounded by red solid lines and blue dotted lines represent the dominated subspaces by the solutions of NIEA and NSGA-II, respectively. The higher hypervolume indicator reflects the better solution quality. The calculated hypervolume indicators and the computation time are summarised in **Table 7**. The hypervolume indicators of NIEA for parts A, B, and C are 14.41, 14.10, and 120.88, respectively. By comparison, the median hypervolume indicators of NSGA-II for parts A, B, and C are 10.69, 10.37, and 68.80, respectively. Thus, it verifies that NIEA performs better than NSGA-II in solution quality.

Although the computation time of NIEA for parts A and B is shorter than that of NSGA-II, its computation time for part C (21970s) is much longer than that of NSGA-II (54.95s). To better compare

the computation time between NIEA and NSGA-II, the algorithms are performed for the other five parts from 9 to 13 actual features, and the results are listed in **Table 8**. According to **Tables 7** and **8**, NIEA performs better than NSGA-II in both solution quality and computation time for the part with fewer than 12 features, thus NIEA is recommended. For the part with 12 or more features, the computation time of NIEA becomes longer than that of NSGA-II, and it is required to make a trade-off between the computation time and the solution quality when selecting an algorithm. While the number of features of a part is increasing, the computation time of NIEA increases sharply whereas the computation time of NSGA-II increases slightly, as reflected in **Tables 7** and **8**. For example, for part B that has 8 features, the computation time of NIEA is only 0.128% (0.0274/21.33) of that of NSGA-II. However, when the number of features increases to 14 such as in part C, the computation time of NIEA becomes 399 (21970/54.95) times more than that of NSGA-II. Hence, when the number of features of a part increases to 14 or more, NSGA-II may be more preferable to get a near-optimal solution set within a tolerable computation time.

**Table 8** Computation time comparison between NIEA and NSGA-II for the other five parts.

## 6. Discussion

The case study has shown that the computation time of NIEA is intolerant when the number of features increases to 14. Although NSGA-II consumes a short computation time, its solution quality is not high. The algorithms with better performance in computation speed and solution quality should be designed and discussed. Research has proved that hybridising the deterministic algorithm with the evolutionary algorithm can improve the algorithm performance [45]. In this paper, the proposed NIEA hybridises with NSGA-II to develop a novel hybrid algorithm for solving our multi-objective feature sequencing problem, and this hybrid algorithm is named Genetic-based Non-dominated Enumeration Algorithm (GNEA). GNEA is an improved enumeration algorithm.

In proposed GNEA, NSGA-II is performed first to obtain the set of optimal or near-optimal PSFPs as an initial upper bound [46] before performing NIEA. With the help of this initial bound, many inferior PSFPs can be efficiently pruned, thereby reducing the computation time of GNEA. As a kind of enumeration algorithm, the solution quality of GNEA is the same as that of NIEA, and the global optimum is guaranteed. Experiments are performed to test the computation time of GNEA.

GNEA is programmed by language C++, and part C with 14 actual features is used as an example. The computation time of GNEA is 5960s, which is 72.87%  $[(21970-5960)/21970]$  shorter than that

of NIEA. It validates that the proposed hybrid algorithm GNEA is an effective deterministic optimisation approach for solving the medium-to-large feature sequencing problem. However, the performance of GNEA is not always better than that of NIEA in computation time. Specifically, the computation time of GNEA is longer than that of NSGA-II because NSGA-II is entirely included in GNEA. As a result, the computation time of GNEA is longer than that of NIEA for the part with fewer than 12 features, and NIEA is still recommended.

## 7. Conclusions and future work

It has been approved that the machining energy consumption can be reduced through sequencing the features of a part at the process planning stage. The single objective model that only minimises the S-MEC has been developed in previous research. However, the S-MT and the S-MD have not been considered. In this article, the conflict between the S-MT and the S-MEC has been verified, and the S-MT and the S-MD have been developed as two new objectives. Further, the developed S-MT and S-MD models are integrated with the existing S-MEC model to obtain the multi-objective model. The time and power data of the machine tool in the model are obtained from experiment measurement. Accordingly, a multi-objective feature sequencing problem, which minimises the S-MT, the S-MD, and the S-MEC, is introduced. To solve this problem, the two algorithms (NIEA and NSGA-II) are proposed as the optimisation approaches that obtain the non-dominated set of optimal solutions. An optimal solution represents a PSFP that results in the optimal trade-off among the three objectives. Because NIEA can always find the global optimum, the results obtained by NSGA-II can be compared and evaluated.

In the case study, the optimal solution sets for three parts with 8, 8, and 14 actual features have been found. According to the optimisation results, NSGA-II usually returns a near-optimal solution set. By comparison, NIEA always returns the global optimal solution set. Therefore, NIEA performs better than NSGA-II in terms of solution quality. Based on the experiment results of the two algorithms for eight parts, NIEA is recommended for the part with fewer than 12 actual features because it consumes the shorter computation time than that of NSGA-II. For the part with 12 or more features, the computation time of NIEA becomes longer than that of NSGA-II, and a trade-off between the computation time and the solution quality should be made when selecting an algorithm. By using the multi-objective feature sequencing approach, 20.51% S-MT, 5.29% S-MD, and 16.66% S-MEC can be reduced. To obtain the global optimum more quickly for the 14-feature part, a novel hybrid algo-



590 rithm GNEA is proposed and compared. The computation time of GNEA is 72.87% shorter than that  
591 of NIEA for the 14-feature part.

592 In this presented paper, the model is only suitable for the parts without the feature intersection. In  
593 real manufacturing circumstance, the feature intersections widely exist in the parts. The model can be  
594 improved for the parts with the feature intersections, through developing the sub-models for the se-  
595 quence-related cutting time, deviation, and energy consumption. Further, the model can be improved  
596 by considering more objectives, such as the machining roughness, tolerance, reliability, and cost, and  
597 the mathematic relationship between these new objectives and the PSFP should be developed. The  
598 single machine environment is a limitation of this presented research. Usually, more than one ma-  
599 chine is required to finish a part, with consuming the time and energy of machine tools for setup  
600 change and machine change. In the next step, the S-MT and the S-MEC in multi-machine environ-  
601 ment should be modelled. For the optimisation approaches, the computation speed of deterministic  
602 algorithms and the solution quality of evolutionary algorithms can be further improved. In the future,  
603 the proposed feature sequencing approach will be combined with the existing energy-aware schedul-  
604 ing approach to promote the energy-aware integrated process planning and scheduling.

## 605 **Acknowledgments**

606 The authors would like to thank the support from the National Natural Science Foundation of China  
607 (Grant No.U1501248), the Nantaihu Innovation Program of Huzhou Zhejiang China, the China  
608 Scholarship Council (Grant No. 201406320033), and the EPSRC EXHUME Project (Efficient X-  
609 sector use of HeterogeneoUs MatErials in Manufacturing) (Grant No. EP/K026348/1).

## 610 **Appendix A. Supplementary data**

611 Supplementary data related to this article can be found at the Supplementary Information (SI).

## 612 **References**

- [1] Liu Y, Dong H, Lohse N, Petrovic S, Gindy N. An investigation into minimising total energy consumption and total weighted tardiness in job shops. *J Clean Prod* 2014; 65: 87-96.
- [2] Hu L, Peng T, Peng C, Tang R. Energy consumption monitoring for the order fulfilment in a ubiquitous manufacturing environment. *Int J Adv Manuf Technol* 2017; 89(9): 3087-100.
- [3] Zhou L, Li J, Li F, Meng Q, Li J, Xu X. Energy consumption model and energy efficiency of machine tools: a comprehensive literature review. *J Clean Prod* 2016; 112: 3721-34.

- [4] Liu F, Xie J, Liu S. A method for predicting the energy consumption of the main driving system of a machine tool in a machining process. *J Clean Prod* 2015; 105: 171-7.
- [5] Cai W, Liu F, Xie J, Zhou X. An energy management approach for the mechanical manufacturing industry through developing a multi-objective energy benchmark. *Energ Convers Manage* 2017; 132: 361-71.
- [6] Calise F, d'Accadia MD, Libertini L, Quiriti E, Vanoli R, Vicidomini M. Optimal operating strategies of combined cooling, heating and power systems: A case study for an engine manufacturing facility. *Energ Convers Manage* 2017; 149: 1066-84.
- [7] Zhang Z, Tang R, Peng T, Tao L, Jia S. A method for minimizing the energy consumption of machining system: integration of process planning and scheduling. *J Clean Prod* 2016; 137: 1647-62.
- [8] Gahm C, Denz F, Dirr M, Tuma A. Energy-efficient scheduling in manufacturing companies: a review and research framework. *Eur J Oper Res* 2016; 248(3): 744-57.
- [9] Yan J, Li L, Zhao F, Zhang F, Zhao Q. A multi-level optimization approach for energy-efficient flexible flow shop scheduling. *J Clean Prod* 2016; 137: 1543-52.
- [10] Dufloy JR, Sutherland JW, Dornfeld D, Herrmann C, Jeswiet J, Kara S, Hauschild M, Kellens K. Towards energy and resource efficient manufacturing: A processes and systems approach. *CIRP Ann-Manuf Technol* 2012; 61(2): 587-609.
- [11] Yan W, Zhang H, Jiang ZG, Hon KKB. Multi-objective optimization of arc welding parameters: the trade-offs between energy and thermal efficiency. *J Clean Prod* 2017; 140: 1842-9.
- [12] Shin S, Woo J, Rachuri S. Energy efficiency of milling machining: Component modeling and online optimization of cutting parameters. *J Clean Prod* 2017; 161: 12-29.
- [13] Hu L, Peng C, Evans S, Peng T, Liu Y, Tang R, Tiwari A. Minimising the machining energy consumption of a machine tool by sequencing the features of a part. *Energy* 2017; 121: 292-305.
- [14] Tseng YJ, Jiang BC. Evaluating multiple feature-based machining methods using an activity-based cost analysis model. *Int J Adv Manuf Technol* 2000; 16(9): 617-23.
- [15] Yan J, Li L. Multi-objective optimization of milling parameters—the trade-offs between energy, production rate and cutting quality. *J Clean Prod* 2013; 52: 462-71.
- [16] Kant G, Sangwan KS. Prediction and optimization of machining parameters for minimizing power consumption and surface roughness in machining. *J Clean Prod* 2014; 83: 151-64.
- [17] Sheng P, Srinivasan M, Kobayashi S. Multi-objective process planning in environmentally conscious manufacturing: a feature-based approach. *CIRP Ann-Manuf Technol* 1995; 44(1): 433-7.
- [18] Newman ST, Nassehi A, Imani-Asrai R, Dhokia V. Energy efficient process planning for CNC machining. *CIRP J Manuf Sci Technol* 2012; 5(2): 127-36.
- [19] Jia S, Yuan Q, Lv J, Liu Y, Ren D, Zhang Z. Therblig-embedded value stream mapping method for lean energy machining. *Energy* 2017; 138: 1081-98.
- [20] Hu L, Liu Y. Minimising energy consumption of tool change and tool path of machining by sequencing features; 2016. Retrieved from <  
[https://www.researchgate.net/publication/306259904\\_Minimising\\_energy\\_consumption\\_of\\_tool\\_change\\_and\\_tool\\_path](https://www.researchgate.net/publication/306259904_Minimising_energy_consumption_of_tool_change_and_tool_path)>. Last visited: 2/8/2016; doi: 10.13140/RG.2.2.20407.11687.

- [21] Hu L, Liu Y, Lohse N, Tang R, Lv J, Peng C, Evans S. Sequencing the features to minimise the non-cutting energy consumption in machining considering the change of spindle rotation speed. *Energy* 2017; 139: 935-46.
- [22] Jin K, Zhang HC, Balasubramaniam P, Nage S. A multiple objective optimization model for environmental benign process planning. In: *Proceedings 2009 IEEE 16th International Conference on Industrial Engineering and Engineering Management*; 2009. p. 869-73.
- [23] Tian G, Zhang H, Feng Y, Wang D, Peng Y, Jia H. Green decoration materials selection under interior environment characteristics: A grey-correlation based hybrid MCDM method. *Renew Sust Energ Rev* 2018; 81: 682-92.
- [24] Cai W, Liu F, Zhang H, Liu P, Tuo J. Development of dynamic energy benchmark for mass production in machining systems for energy management and energy-efficiency improvement. *Appl Energ* 2017; 202: 715-25.
- [25] Yin R, Cao H, Li H, Sutherland JW. A process planning method for reduced carbon emissions. *Int J Comput Integ M* 2014; 27(12): 1175-86.
- [26] Srinivasan M, Sheng P. Feature based process planning in environmentally conscious machining–Part 2: macroplanning. *Robot Cim-Int Manuf* 1999; 15(3): 271-81.
- [27] Deb K, Pratap A, Agarwal S, Meyarivan TAMT. A fast and elitist multiobjective genetic algorithm: NSGA-II. *IEEE T Evolut Comput* 2002; 6(2): 182-97.
- [28] Li C, Chen X, Tang Y, Li L. Selection of optimum parameters in multi-pass face milling for maximum energy efficiency and minimum production cost. *J Clean Prod* 2017; 140: 1805-18.
- [29] Lu C, Gao L, Li X, Chen P. Energy-efficient multi-pass turning operation using multi-objective backtracking search algorithm. *J Clean Prod* 2016; 137: 1516-31.
- [30] Lv JX, Tang RZ, Jia S, Liu Y. Experimental study on energy consumption of computer numerical control machine tools. *J Clean Prod* 2016; 112: 3864-74.
- [31] He K, Tang R, Zhang Z, Sun W. Energy consumption prediction system of mechanical processes based on empirical models and computer-aided manufacturing. *J Comput Inf Sci Eng* 2016; 16(4): 041008.
- [32] Lv JX. Research on Energy Supply Modeling of Computer Numerical Control Machine Tools for Low Carbon Manufacturing [dissertation]. Hangzhou: Zhejiang University; 2014 [in Chinese].
- [33] Gara S, Bouzid W, Amar MB, Hbaieb M. Cost and time calculation in rough NC turning. *Int J Adv Manuf Technol* 2009; 40(9): 971-81.
- [34] Lee DH, Kiritsis D, Xirouchakis P. Branch and fathoming algorithms for operation sequencing in process planning. *Int J Prod Res* 2001; 39(8): 1649-69.
- [35] Wiener R. Branch and bound implementations for the traveling salesperson problem - part 1: a solution with nodes containing partial tours with constraints. *J Obj Technol* 2003; 2(2): 65-86.
- [36] Martinez-Legaz JE. Lexicographical order and duality in multiobjective programming. *Eur J Oper Res* 1988; 33(3): 342-8.
- [37] Jain V, Sachdeva G. Energy, exergy, economic (3E) analyses and multi-objective optimization of vapor absorption heat transformer using NSGA-II technique. *Energ Convers Manage* 2017; 148: 1096-113.

- [38] Bolaños R, Echeverry M, Escobar J. A multiobjective non-dominated sorting genetic algorithm (NSGA-II) for the multiple traveling salesman problem. *Decis Sci Lett* 2015; 4(4): 559-68.
- [39] Forrest S. Genetic algorithms: principles of natural selection applied to computation. *Science* 1993; 261(5123): 872-8.
- [40] Blickle T, Thiele L. A comparison of selection schemes used in evolutionary algorithms. *Evol Comput* 1996; 4(4): 361-94.
- [41] Goldberg DE, Lingle R. Alleles, loci, and the traveling salesman problem. In: *Proceedings of the First International Conference on Genetic Algorithms and Their Applications*; 1985. p.154-9.
- [42] Ruiz R, Maroto C, Alcaraz J. Two new robust genetic algorithms for the flowshop scheduling problem. *Omega-Int J Manage S* 2006; 34(5): 461-76.
- [43] Al-Sahib NKA, Abdulrazzaq HF. Tool path optimization of drilling sequence in CNC machine using genetic algorithm. *Innov Syst Des Eng* 2014; 5(1): 15-26.
- [44] Auger A, Bader J, Brockhoff D, Zitzler E. Hypervolume-based multiobjective optimization: Theoretical foundations and practical implications. *Theor Comput Sci* 2012; 425: 75-103.
- [45] French AP, Robinson AC, Wilson JM. Using a hybrid genetic-algorithm/branch and bound approach to solve feasibility and optimization integer programming problems. *J Heuristics* 2001; 7(6): 551-64.
- [46] Peng C, Peng T, Tang R, Zhang Y, Hu L. Minimizing energy consumption and tardiness fine in a mixed-flow shop environment: a scheduling approach; 2017. Retrieved from < [https://www.researchgate.net/publication/321162151\\_Minimizing\\_energy\\_consumption\\_and\\_tardiness\\_fine\\_in\\_a\\_mixed-flow\\_shop\\_environment\\_a\\_scheduling\\_approach](https://www.researchgate.net/publication/321162151_Minimizing_energy_consumption_and_tardiness_fine_in_a_mixed-flow_shop_environment_a_scheduling_approach) >. Last visited: 20/11/2017; doi: 10.13140/RG.2.2.17859.91682.

**Table 1** Spindle rotation speeds for the features in parts A, B, and C.

The $i$ -th feature in part A	The $i$ -th feature in part B	The $i$ -th feature in part C	Spindle rotation speed [rpm]
$F_1$	$F_1, F_3$	$F_1, F_3$	500
$F_2$	$F_2, F_4$	$F_2, F_4$	550
$F_3$	$F_5, F_6$	$F_5$	700
$F_4$	$F_7, F_8$	$F_6$	650
$F_5$		$F_7, F_8$	600
$F_6$		$F_9, F_{10}$	800
$F_7$		$F_{11}, F_{12}$	450
$F_8$		$F_{13}, F_{14}$	750

620  
621  
622

**Table 2** S-NT for 81 pairs of features in part A.

Time [s]	$F_1$	$F_2$	$F_3$	$F_4$	$F_5$	$F_6$	$F_7$	$F_8$	$F_9$
$F_0$	0.575	0.880	0.785	0.855	0.660	0.805	1.095	1.200	$\infty$
$F_1$	$\infty$	0.305	0.210	0.505	0.185	0.455	0.756	0.850	0.582
$F_2$	0.306	$\infty$	0.205	0.200	0.230	0.250	0.461	0.545	0.887
$F_3$	0.213	0.207	$\infty$	0.386	0.126	0.325	0.668	0.720	0.794
$F_4$	0.507	0.201	0.385	$\infty$	0.321	0.130	0.283	0.345	0.864
$F_5$	0.186	0.231	0.125	0.320	$\infty$	0.270	0.592	0.665	0.668
$F_6$	0.459	0.253	0.326	0.132	0.273	$\infty$	0.365	0.406	0.816
$F_7$	0.755	0.460	0.665	0.280	0.590	0.360	$\infty$	0.205	1.101
$F_8$	0.853	0.548	0.721	0.346	0.667	0.405	0.209	$\infty$	1.210

623  
  
624  
  
625

626  
627  
628  
  
  
629  
  
630  
631

**Table 3** S-ND for 81 pairs of features in part A.

Deviation [μm]	$F_1$	$F_2$	$F_3$	$F_4$	$F_5$	$F_6$	$F_7$	$F_8$	$F_9$
$F_0$	120.93	204.02	164.84	213.10	153.05	188.22	246.98	279.02	$\infty$
$F_1$	$\infty$	84.85	43.91	105.11	38.08	86.31	152.07	175.57	0
$F_2$	84.85	$\infty$	43.91	43.91	51.48	51.48	96.57	105	0
$F_3$	43.91	43.91	$\infty$	76	26.42	67.07	128.66	144.68	0
$F_4$	105.11	43.91	76	$\infty$	67.07	26.42	53.60	70.52	0
$F_5$	38.08	51.48	26.42	67.07	$\infty$	50	115.43	137.57	0
$F_6$	86.31	51.48	67.07	26.42	50	$\infty$	65.76	91.79	0
$F_7$	152.07	96.57	128.66	53.60	115.43	65.76	$\infty$	38.08	0
$F_8$	175.57	105	144.68	70.52	137.57	91.79	38.08	$\infty$	0

632  
633  
634  
  
  
635  
  
636  
637

**Table 4** S-NEC for 81 pairs of features in part A.

Energy [J]	$F_1$	$F_2$	$F_3$	$F_4$	$F_5$	$F_6$	$F_7$	$F_8$	$F_9$
$F_0$	1065.33	1624.95	1435.98	1767.06	1330.39	1711.47	1973.30	2316.91	$\infty$
$F_1$	$\infty$	556.07	358.34	788.00	302.77	723.91	1027.85	1323.86	965.80
$F_2$	539.45	$\infty$	368.00	343.83	338.89	438.89	670.02	770.05	1497.85
$F_3$	274.29	303.94	$\infty$	495.99	166.65	521.41	862.89	1012.12	1210.50
$F_4$	732.75	303.73	517.21	$\infty$	468.08	241.95	369.65	540.18	1576.99
$F_5$	265.85	320.30	210.69	487.93	$\infty$	423.28	769.88	1026.68	1173.12
$F_6$	588.21	319.80	472.50	167.03	327.08	$\infty$	440.08	639.07	1407.35
$F_7$	1040.89	701.29	956.58	445.90	819.09	599.01	$\infty$	357.04	1898.72
$F_8$	1225.92	685.17	990.69	494.74	963.61	663.50	224.78	$\infty$	2053.42



**Table 5** The results obtained by BTT and NIEA for parts A, B, and C.

	BTT		NIEA		
	S-MT [s]	S-MEC [J]	The set of the optimal PSFPs	S-MT [s]	S-MEC [J]
Part A	4.022	6321.99	$F_0 - F_6 - F_8 - F_7 - F_4 - F_2 - F_3 - F_5 - F_1 - F_9$	3.000	5091.26
			$F_0 - F_1 - F_5 - F_3 - F_2 - F_4 - F_7 - F_8 - F_6 - F_9$	3.001	5024.09
			$F_0 - F_1 - F_5 - F_3 - F_2 - F_4 - F_8 - F_7 - F_6 - F_9$	3.022	4997.88
			$F_0 - F_1 - F_3 - F_2 - F_4 - F_7 - F_8 - F_6 - F_5 - F_9$	3.026	4961.82
			$F_0 - F_1 - F_3 - F_2 - F_4 - F_8 - F_7 - F_6 - F_5 - F_9$	3.047	4935.61
			$F_0 - F_1 - F_3 - F_2 - F_8 - F_7 - F_4 - F_6 - F_5 - F_9$	3.097	4910.49
Part B	3.737	5790.27	$F_0 - F_1 - F_6 - F_2 - F_7 - F_3 - F_8 - F_4 - F_5 - F_9$	2.499	4235.01
Part C	6.728	9871.92	$F_0 - F_7 - F_1 - F_8 - F_2 - F_9 - F_{10} - F_{13} - F_{12} - F_3 - F_{11} - F_{14} - F_6 - F_4 - F_5 - F_{15}$	3.909	6547.28
			$F_0 - F_1 - F_7 - F_8 - F_2 - F_9 - F_{10} - F_{13} - F_{12} - F_3 - F_{11} - F_{14} - F_6 - F_4 - F_5 - F_{15}$	3.913	6288.12
			$F_0 - F_1 - F_7 - F_8 - F_2 - F_9 - F_{10} - F_3 - F_{13} - F_{12} - F_{11} - F_{14} - F_6 - F_4 - F_5 - F_{15}$	3.980	6121.71
			$F_0 - F_1 - F_7 - F_8 - F_2 - F_9 - F_{10} - F_3 - F_{12} - F_{13} - F_{14} - F_{11} - F_6 - F_4 - F_5 - F_{15}$	4.095	6085.46

644  
645  
646

**Table 6** The solutions obtained by NIEA for the multi-objective model of part A.

The set of optimal feature sequences of part A	S-MT [s]	S-MEC [J]	S-MD [ $\mu\text{m}$ ]
$F_0-F_6-F_8-F_7-F_4-F_2-F_3-F_5-F_1-F_9$	3.000	5091.26	524.01
$F_0-F_1-F_5-F_3-F_2-F_4-F_7-F_8-F_6-F_9$	3.001	5024.09	456.72
$F_0-F_1-F_5-F_3-F_2-F_4-F_8-F_7-F_6-F_9$	3.022	4997.88	447.61
$F_0-F_1-F_3-F_2-F_4-F_7-F_8-F_6-F_5-F_9$	3.026	4961.82	486.13
$F_0-F_1-F_3-F_2-F_4-F_8-F_7-F_6-F_5-F_9$	3.047	4935.61	477.02
$F_0-F_1-F_5-F_3-F_2-F_8-F_7-F_4-F_6-F_9$	3.072	4972.76	452.44
$F_0-F_1-F_3-F_2-F_8-F_7-F_4-F_6-F_5-F_9$	3.097	4910.49	481.85
$F_0-F_1-F_5-F_3-F_2-F_6-F_4-F_8-F_7-F_9$	3.129	5152.33	415.84
$F_0-F_1-F_5-F_6-F_7-F_8-F_4-F_2-F_3-F_9$	3.146	4965.48	471.19
$F_0-F_1-F_5-F_3-F_2-F_6-F_4-F_7-F_8-F_9$	3.172	5268.75	398.92
$F_0-F_1-F_5-F_6-F_4-F_7-F_8-F_2-F_3-F_9$	3.197	4948.77	476.02

647  
648  
649

650

651

652

**Table 7** Performance comparison between NIEA and NSGA-II for parts A, B, and C.

Part names		Part A	Part B	Part C
Number of actual features		8	8	14
NIEA	Hypervolume indicator	14.41	14.10	120.88
	Computation time [s]	0.0286	0.0274	21970
NSGA-II	Maximum hypervolume indicator	11.08	14.10	99.34
	Median hypervolume indicator	10.69	10.37	68.80
	Computation time [s]	20.37	21.33	54.95

653

654

655

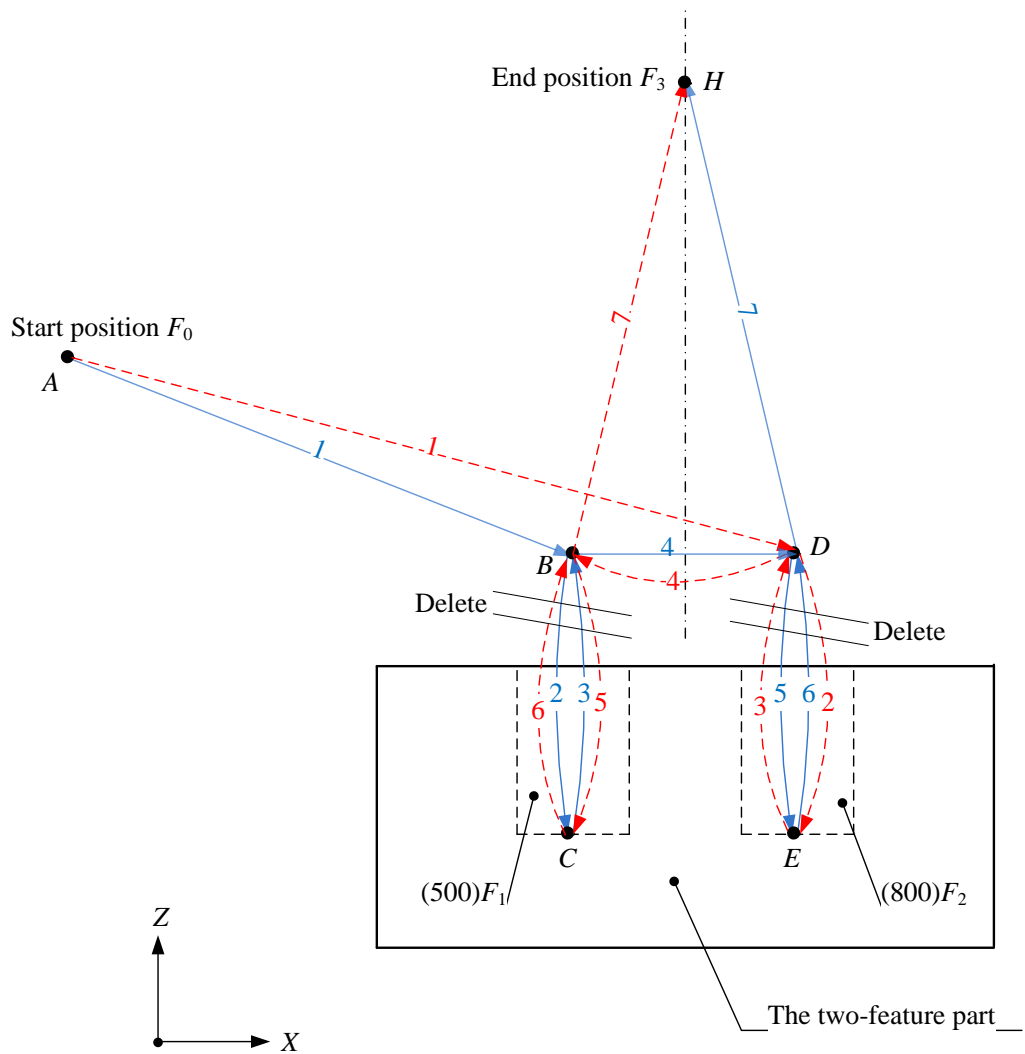
656  
657  
658  
  
659  
  
660  
661

**Table 8** Computation time comparison between NIEA and NSGA-II for the other five parts.

Part names		Part D	Part E	Part F	Part G	Part H
Number of actual features		9	10	11	12	13
Computation time [s]	NIEA	0.297	1.048	10.42	121.2	1554
	NSGA-II	22.71	23.73	24.86	25.14	27.35

662

663



664

665

**Fig. 1.** A two-feature part that has two possible processing sequences.

666

667

668

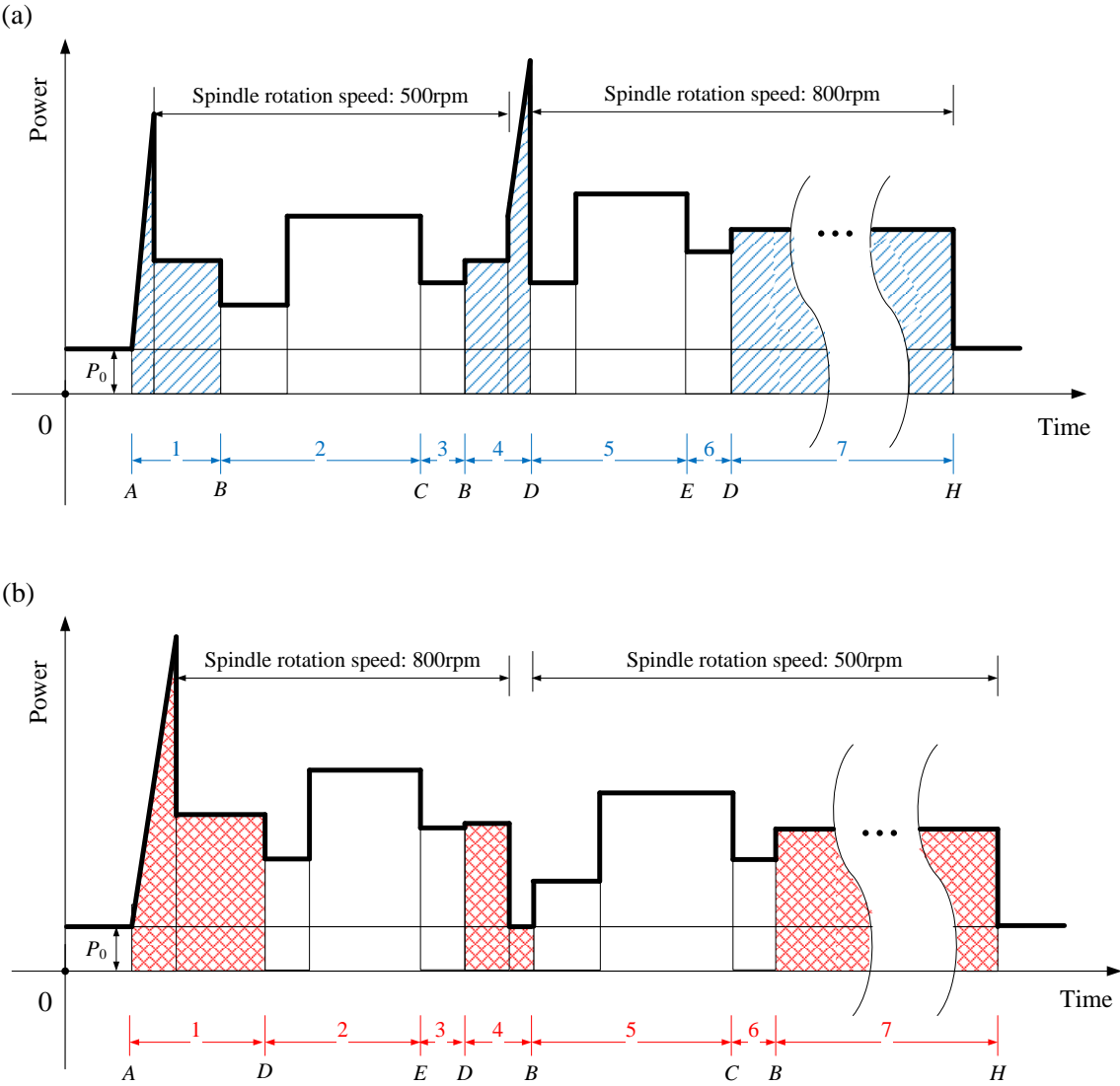
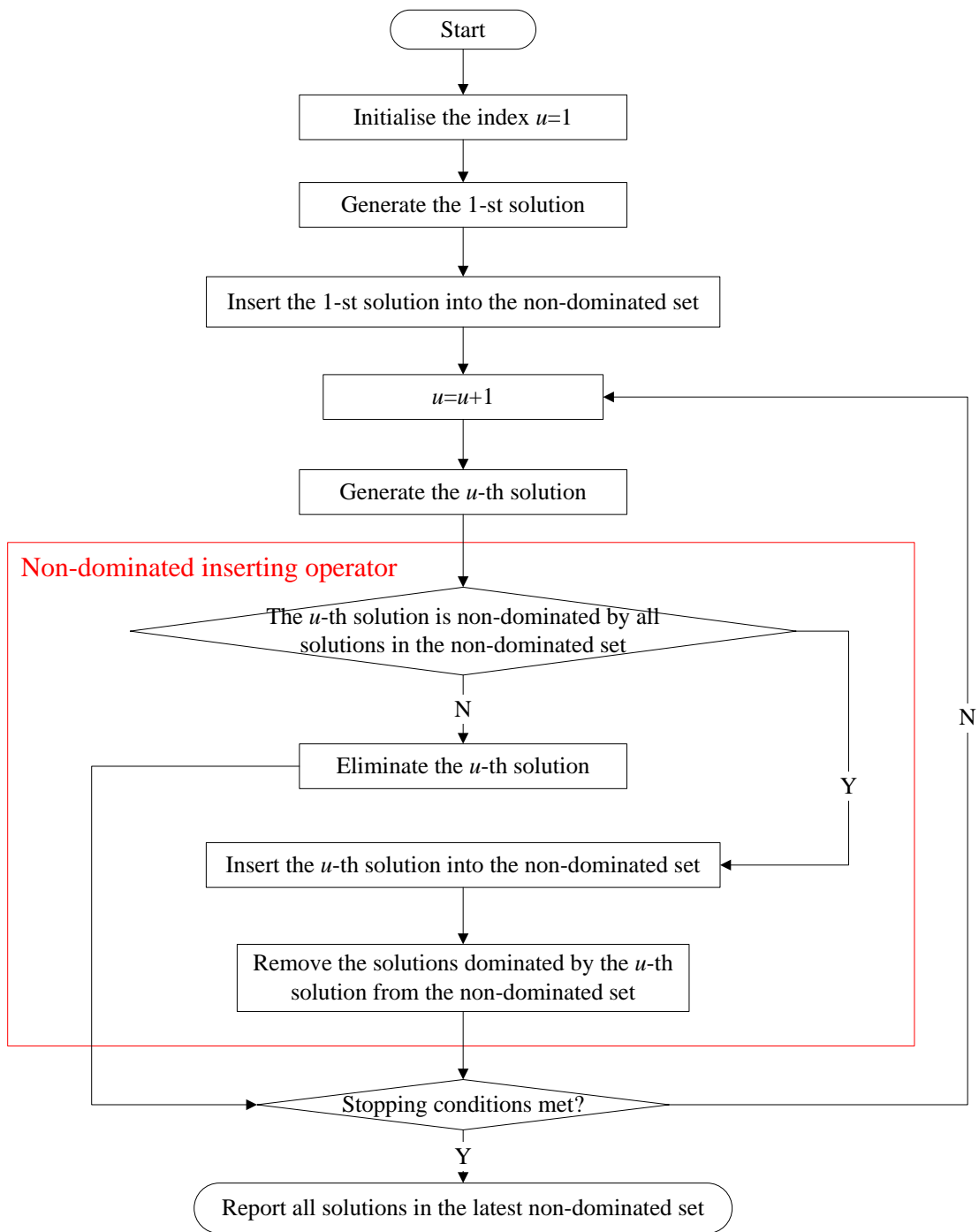


**Fig. 2.** Power profiles of two different sequences: (a)  $F_0$ - $F_1$ - $F_2$ - $F_3$ ; (b)  $F_0$ - $F_2$ - $F_1$ - $F_3$ .

675



676

677

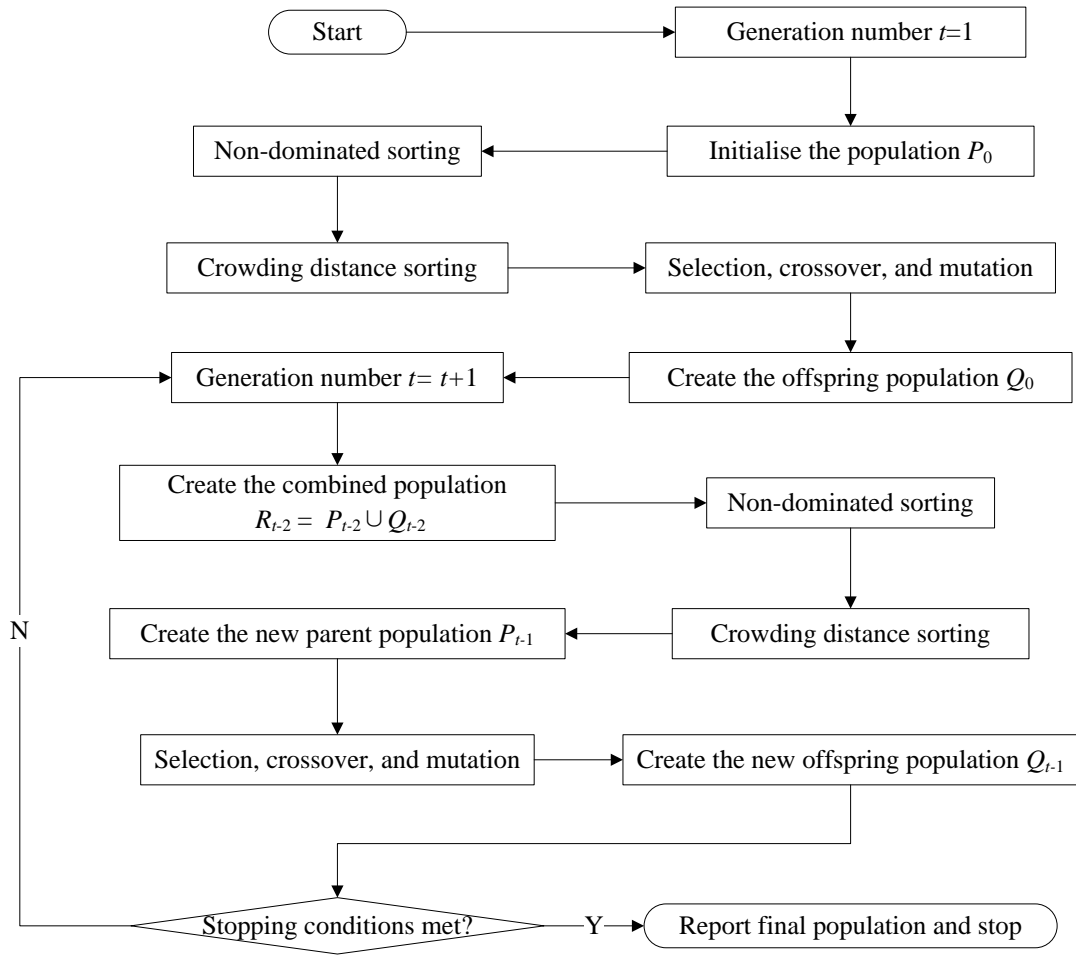
**Fig. 3.** Flowchart of NIEA.

678

679

680

681



682

683

**Fig. 4.** Flowchart of NSGA-II.

684

685



686

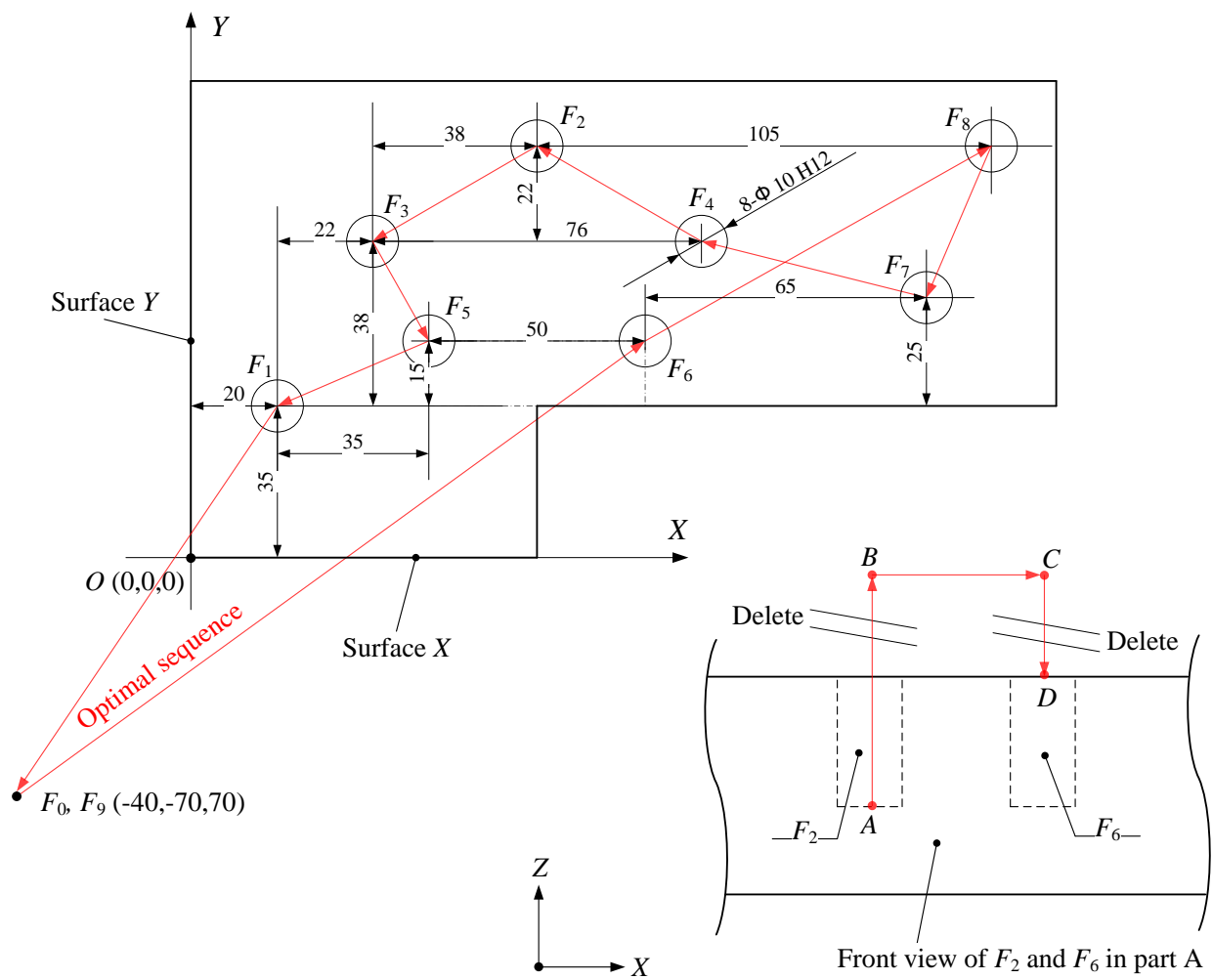


**Fig. 5.** Part A with 8 actual features and 2 virtual features.

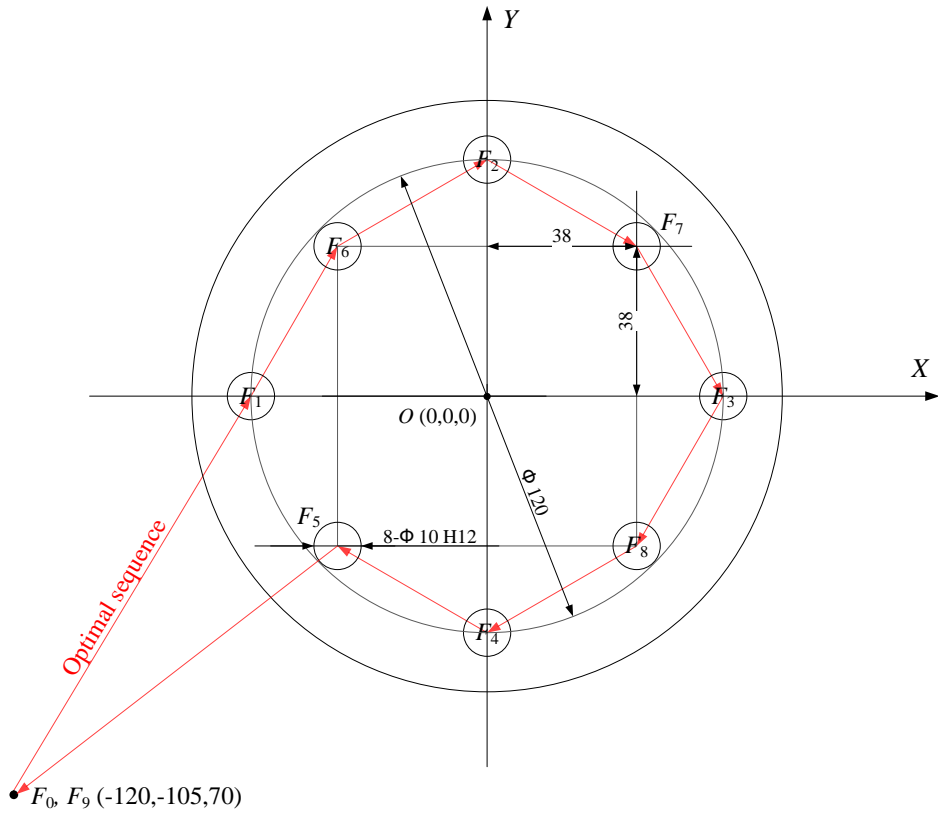
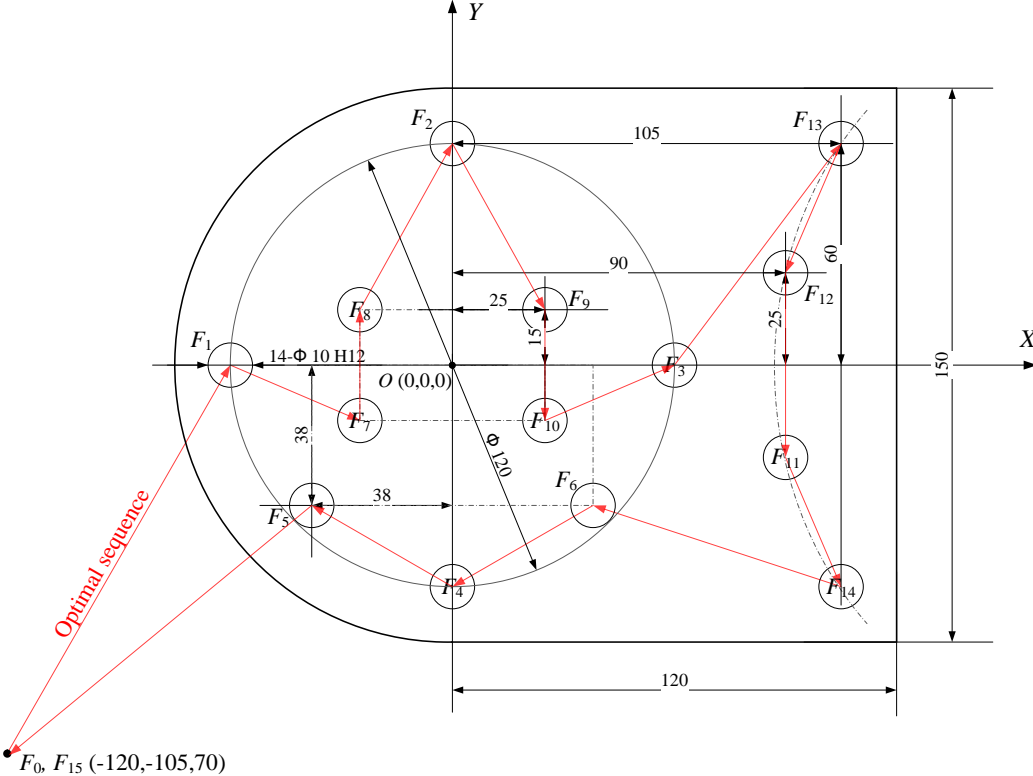


**Fig. 6.** Part B with 8 actual features and 2 virtual features.

697



698

699

700

701

**Fig. 7.** Part C with 14 actual features and 2 virtual features.

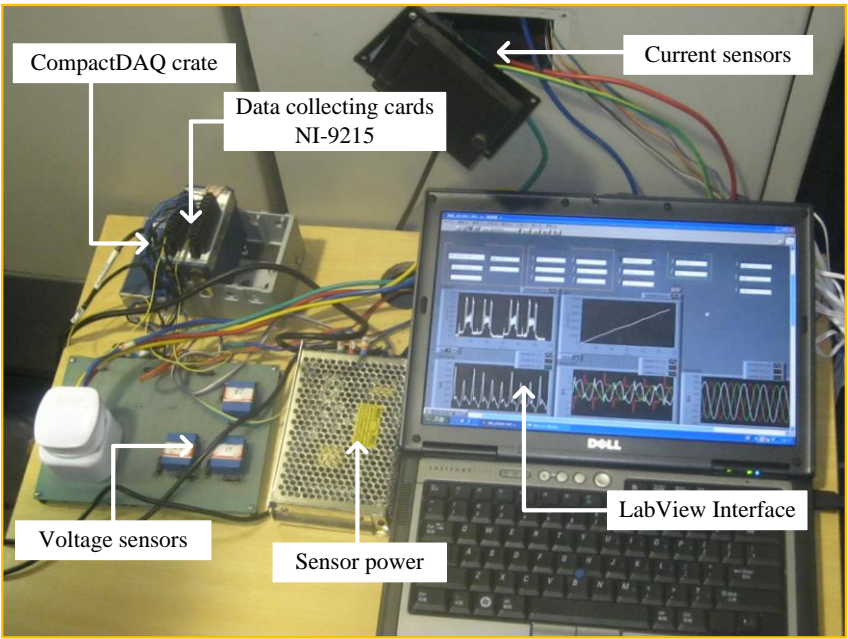
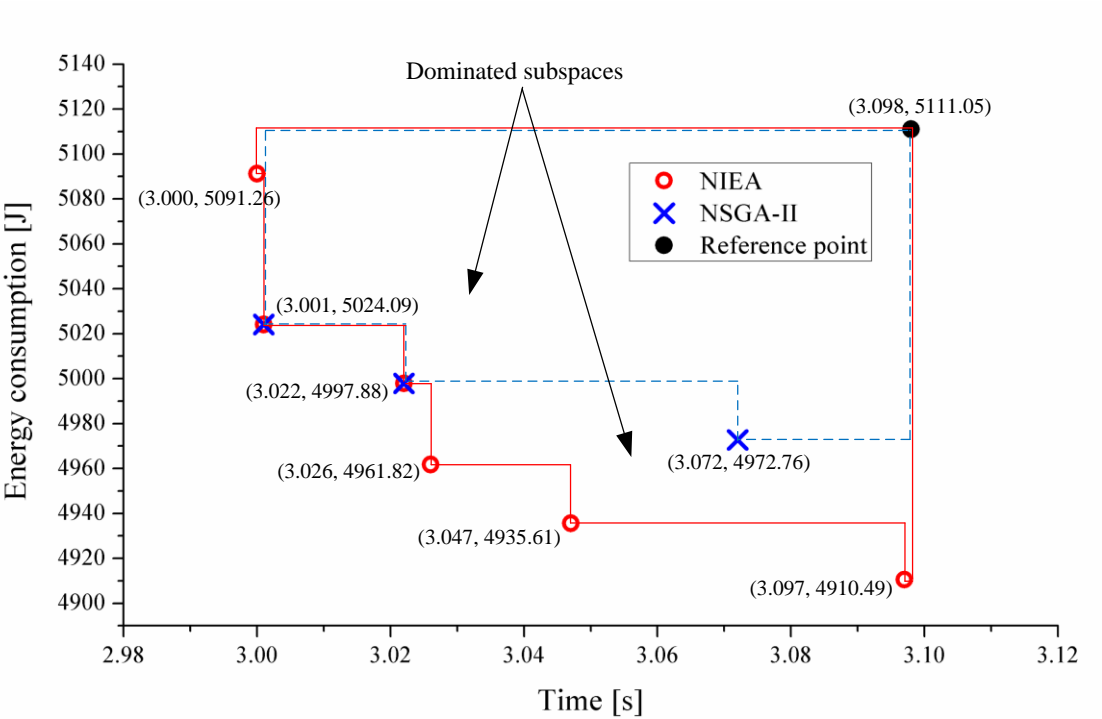


**Fig. 8.** Diagram of the experiment setup for power data acquisition.

708



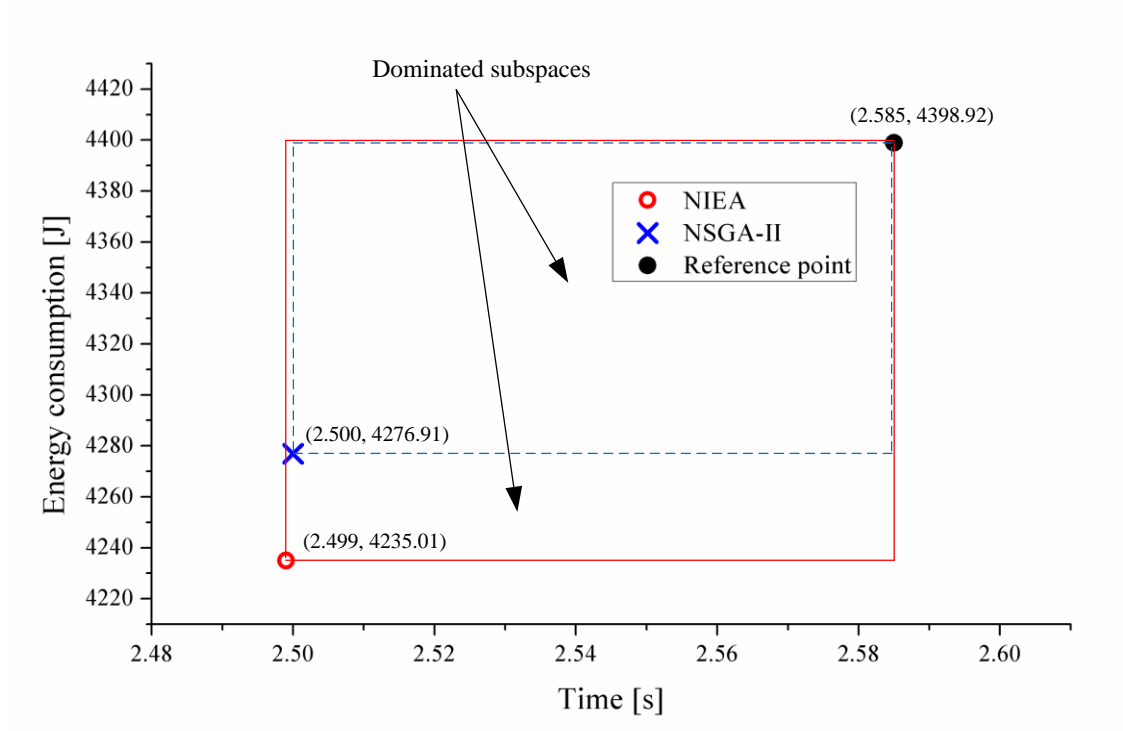
709

710 **Fig. 9.** Comparison of solution quality between NIEA and NSGA-II for part A.

711

712

713



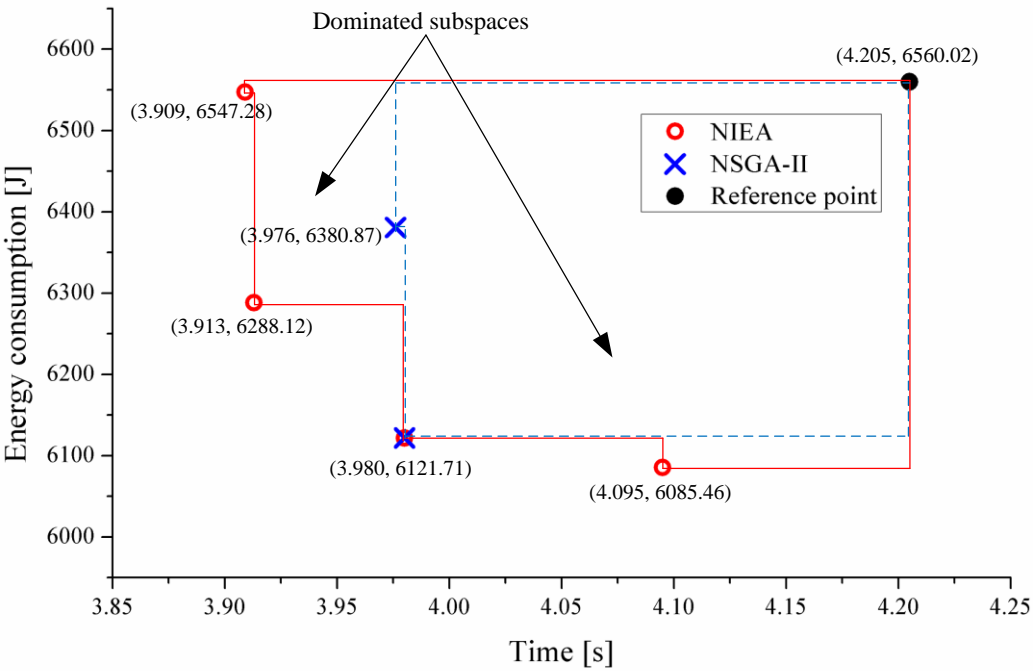
714

715 **Fig. 10.** Comparison of solution quality between NIEA and NSGA-II for part B.

716

717

718



719

720 **Fig. 11.** Comparison of solution quality between NIEA and NSGA-II for part C.

721

722

723